치의과학박사 학위논문

Flexural test as an alternative to tensile test for bond strength of resin cement to zirconia: statistical and finite element analyses

지르코니아 세라믹에 대한 레진 시멘트의 굽힘접착강도 시험을 통한 인장접착강도 시험에 대한 대안 연구 : 통계 및 유한요소법적 해석

2022년 2월

서울대학교 대학원

치의과학과 치과보존과 전공

신 유 진

Flexural test as an alternative to tensile test for bond strength of resin cement to zirconia: statistical and finite element analyses

지도교수 조 병 훈

이 논문을 치의과학박사 학위논문으로 제출함

2022년 2월

서울대학교 대학원

치의과학과 치과보존과 전공

신 유 진

신유진의 박사학위논문을 인준함

2022년 1월

위 원 장 _____ (인)

부위원장 _____ (인)

위 원 _____ (인)

위 원 _____ (인)

위 원 _____ (인)

Abstract

Objective: There has been technical difficulties in measuring the bond strengths between brittle dental substrates and materials, especially in preparing specimens. This study evaluated the validity of the relatively easy flexural bond strength (FBS) test in measuring bond strength of resin cement to zirconia as an alternative to the cumbersome tensile bond strength (TBS) and micro-tensile bond strength (MTBS) tests.

Material and Methods: The FBS and TBS of resin cement to zirconia were measured experimentally after three surface treatments on a zirconia ceramic: air abrasion only (A), conditioning with Single Bond Universal (U) after air abrasion, and conditioning with Z-Prime Plus (Z) after air abrasion. The data were investigated using two-way analysis of variance (ANOVA), Weibull statistics, and a theoretical simulation. In addition, using a finite element analysis (FEA), the validity of the FBS test as an alternative to the TBS was verified again by comparing the stress distribution within the virtual specimens in both test configurations.

Results: In both the FBS and TBS tests, the experimental data were consistent and quantitatively similar. First, according to ANOVA, the U group showed the highest bond strengths in both tests, followed by the Z group and the A group. In each surface treatment group, the FBS was higher than the TBS. Second, the Weibull fitting showed the same order of strength in both tests (A < Z < U) and in all surface treatment groups (FBS > TBS). Third, the theoretical ratios calculated from the Weibull moduli agreed well with the

experimental ratios of the FBS to the TBS. Finally, a similar pattern in stress distributions within both the virtual models were also confirmed by the FEA.

Conclusion: The FBS test can be an alternative to the TBS and MTBS tests in measuring the bond strength of brittle resin cement to zirconia.

Keywords: Adhesive dentistry; finite element analysis; flexural strength; statistical data analysis; tensile strength; zirconia ceramic

Student number: 2014-30704

Table of Contents

List of Figures

List of Tables

Chapter 1. Introduction

1.1. Study Background

Bond strength test is widely used to evaluate the performance of adhesives or resin cements used for dental substrates (enamel and dentin) and dental materials (Bouillaguet et al., 2003; Münchow et al., 2013). Tensile bond strength (TBS) test, shear bond strength (SBS) test, and flexural bond strength (FBS) test are commonly used to evaluate the performance of brittle dental adhesives. Because of the brittle nature of dental substrates and dental materials, two issues are critical for bond strength tests. One is the complicated protocol of each test and the other is the test procedure, since it is difficult to prepare and fix the specimen on the testing jig. Many researchers have tried to develop a standardized protocol for bond strength testing (Sano et al., 1994; Silva et al., 2006; Van Noort et al., 1989; Van Noort et al., 1991).

During the last few decades, the micro-tensile bond strength (MTBS) test has been widely accepted as a standardized protocol for evaluating bond strength in the dental field, in that it has advantages in implementing ideal test mechanics in the sense of uniaxial tensile load, obtaining the actual bond strength and failure mode associated with the adhesive layer, obtaining the

exact bond strength of a small targeted area in the selected site, preparing more specimens from a limited number of obtainable human teeth, etc (Armstrong et al., 2017; Dobi and Junghans, 1999; Gianola and Eberl, 2009; Inoue et al., 2001; Visintini et al., 2008; Zhang et al., 2010). As it became difficult to obtain human teeth for adhesion tests, the MTBS test using a small bonded area ($\leq$ 1.0 mm^2) by cutting a bonded tooth sample into multiple test specimens was proposed, in which bond strength values were increased and failures were guided mostly within the adhesive layer due to decreased probability of flaw distributions and improved force direction perpendicular to the bonded surface, respectively (Sano et al., 1994). However, in the MTBS test, the testing specimens need to be cut from bonded samples. Because of the brittle characteristics of the adhesion and substrate materials, the MTBS test in dentistry requires very difficult and labor-intensive procedures in preparing the test specimens (cutting and grooving) and measuring their bond strengths (aligning the specimen on the testing jig) (Ferrari et al., 2002). Because immediate cutting of the bonded samples into each testing specimen causes too much loss of specimens (Goracci et al., 2004; Kim et al., 2015), the cutting and measuring procedures should be performed after 24 hours from bonding. In addition, there still remain variations in data sets among bonded samples (inter-sample variations) even within the same group (Loguercio et al., 2005).

In order to overcome the difficulties in specimen preparation, an alternative method has been sought to substitute the conventional bond strength tests. The micro-shear bond strength (MSBS) test was proposed as a substitute for the MTBS test (El Zohairy et al., 2010; Kim et al., 2014; Kim et al., 2015; Münchow et al., 2013; Shimada et al., 2002). However, the SBS and MSBS tests have their own problems, resulting in cohesive fracture of the substrate, which is caused by the mechanics of the shear tests (Fornazari et al., 2020; Zhang et al., 2010). In contrast, specimen preparation for the FBS test is relatively easy. Thus, the FBS test may be preferable to the SBS and TBS tests. For single (unbonded) brittle materials, flexural testing has been used rather than tensile testing (Al-Zain and Marghalani, 2020; Eshmawi et al., 2018; Nakamura et al., 2012). However, in order to adopt the FBS test as an alternative to the TBS test, it is necessary to conduct a rigorous evaluation for the performance of the tests in measuring bond strength of brittle dental adhesives.

In this study, to verify the validity of the FBS test, the FBS values of a resin cement (RelyX Ultimate, 3M ESPE, St Paul, MN, USA) to zirconia (IPS e.max ZirCAD, Ivoclar Vivadent, Schaan, Liechtenstein) were statistically compared with the values obtained from TBS testing. As an experimental variable, the surface treatment with sandblasting could play an important role

in zirconia bonding (Inokoshi et al., 2021; Thammajaruk et al., 2018). To determine whether the bond strengths would show consistent results in both the TBS and FBS tests for three kinds of surface treatments—air abrasion only, conditioning with Single Bond Universal after air abrasion, and conditioning with Z-Primer Plus after air abrasion—the bond strength values were measured after these three surface treatments using both test methods.

To investigate the validity of the FBS test as an alternative to the TBS and MTBS tests, three statistical analyses that are a two-way analysis of variance (ANOVA), Weibull statistics, and a theoretical simulation, were used in this study, and additionally, a finite element analysis (FEA) was used to confirm the results of the statistical analyses. First, the mean values and standard deviations of the bond strength tests of the experimental groups were calculated and compared using ANOVA. Second, the Weibull distribution can also be used to analyze the characteristics of strength values in brittle materials, especially in dental adhesives (Weibull, 1939; Weibull, 1951). The Weibull statistics can describe the strength of brittle materials fairly well (Afferrante et al., 2006; Bermejo and Danzer, 2014; Laurencin et al., 2008; Quinn, 2003; Quinn and Quinn, 2010). Afferrante et al. (2006) suggested that the Weibull modulus should not be considered as a 'material constant,' as it varies depending on the distribution of cracks, their distances, and interactions with

the geometry of the cracks and stress field. Quinn and Quinn (2010) reviewed the use of the Weibull statistics for reporting the strength of dental materials and concluded that Weibull analysis has a strong theoretical basis and can be of particular value in dental applications. Therefore, the Weibull statistics has been used to analyze modulus and characteristic strength from the viewpoint of crack distribution to evaluate brittle dental materials and dental adhesives. Third, based on the Weibull theory, researchers became interested in comparing strength ratios among different test configurations. Leguillon et al. (2015) compared flexural and tensile strength in brittle materials. Bhushan et al. (2016) derived semi-analytical expressions for effective volume and effective surface for a cylindrical bar loaded in flexure and calculated the strength scaling ratio between two different loading configurations. In this study, for additional verification of the validity of the FBS test, the ratios of the FBS to the TBS obtained from experiments were also compared with those obtained from a theoretical simulation.

Finite element analysis (FEA) is widely used to analyse and compare the stress distribution in a structure on a virtual model. The FEA was applied to understand the problems of shear test and tensile test in the field of dentistry. (Ghassemieh, 2008; Van Noort et al., 1991; Versluis et al., 1997) In this study, the FEA was used to re-verify the statistical analysis results of the measured

FBS and TBS values. To this end, the bonded specimen was modelled with the eight-node solid elements and its elastic behaviour was analysed to show graphically that it would undergo similar stress distribution under both loading conditions, meaning that the maximum stress would be exerted at about the same region regardless of the loading conditions.

1.2. Purpose of Thesis

The purpose of this study was to evaluate the validity of the relatively easy FBS test as an alternative to the cumbersome TBS and MTBS tests. For the purpose, after three kinds of surface treatments were applied on a zirconia ceramic, the FBS and TBS values of a resin cement to zirconia were measured experimentally. To confirm whether the FBS test yielded the same results as the TBS test from the viewpoint of quantitative ordering, the data were statistically investigated using two-way ANOVA, Weibull statistics, and a theoretical simulation, and additionally verified using an FEA again.

Chapter 2. Materials and Methods

2.1 Zirconia specimen preparation

All the materials used in this study are summarized in **Table 1**. Zirconia specimens were prepared according to the following procedures (**Fig. 1**). IPS e.max ZirCAD blocks (Ivoclar Vivadent, Schaan, Liechtenstein) were sectioned using a water-cooled low-speed diamond saw (Diamond Wafering Blade series 15LC Diamond; Buehler, Lake Bluff, IL, USA) to obtain 19 mm × 17 mm × 3.2 mm cuboids. The cuboids were sintered in a furnace (Programat CS4, Ivoclar Vivadent) according to the manufacturer's instructions. After sintering, 180 zirconia sticks (2 mm × 2 mm × 12.5 mm) (± 0.03 mm) were fabricated by cutting and grinding the sintered cuboids.

Table 1. Information on the materials used in this study

Product	Type of material	Manufacturer	Composition
IPS e.max ZirCAD	Y-TZP	Ivoclar Vivadent Schaan, Liechtenstein	ZrO_2, Y_2O_3, HfO_2, Al_2O_3, other oxide ceramics
Z-Prime Plus	Zirconia-alumina-metal primer	BISCO Schaumburg, IL, USA	10-MDP, BPDM, HEMA, ethanol
Single Bond Universal	One-step adhesive containing MDP	3M ESPE St Paul, MN, USA	MDP, Bis-GMA, HEMA, DMA, methacrylate functional copolymer, filler, ethanol, water, silane
RelyX Ultimate	Dual cure composite resin cement	3M ESPE St Paul, MN, USA	Base paste: methacrylate monomers, radiopaque silanized fillers, initiator, stabilizer, rheological additives
			Catalyst paste: methacrylate monomers, radiopaque alkaline (basic) fillers, initiator, stabilizer, pigments, rheological additives, fluorescence dye, dark cure activator for Scotchbond Universal

MDP, 10-methacryloyloxy-decyl dihydrogenphosphate; BPDM, biphenyl demethacrylate; HEMA, 2-hydroxyethyl methacrylate; Bis-GMA, bisphenol-A-diglycidylmethacrylate; DMA, aliphatic dimethacrylate.

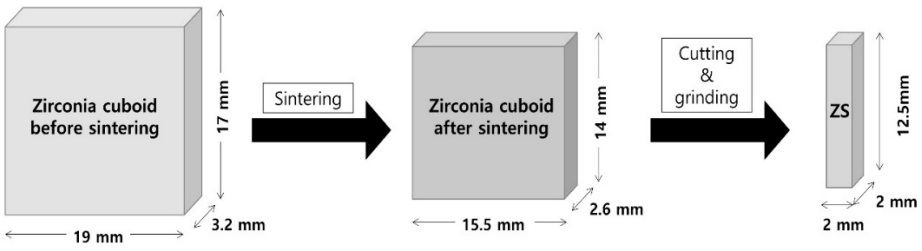

Fig. 1. Schematic view and dimensions of zirconia specimen preparation. Zirconia sticks (ZS) were fabricated using sintered zirconia cuboids.

The square-shaped surfaces for bonding of all zirconia specimens were subjected to air-abrasion with 50 μm Al_2O_3 particles. The nozzle was held perpendicular to the surface from a distance approximately 10 mm for 20 s at a pressure of 3 bar (Qeblawi et al., 2010; Attia et al.,2011). Air-abraded surfaces were observed under microscopy to identify any missed spots. The specimens were ultrasonically cleaned in distilled water for 5 min and dried under vacuum for 24 h.

2.2 Surface treatment procedure

The zirconia specimens were randomly divided into three groups of 60 specimens each according to the different surface treatments. The air abrasion group, represented by the letter A, received no further treatment following air abrasion. The second group, represented by the letter U, was conditioned with Single Bond Universal according to the manufacturer's instructions after air abrasion. In the third group, represented by the letter Z, Z-Prime Plus was applied according to the manufacturer's instructions after air abrasion. **Table 2** presents the letter codes and corresponding surface treatment/test methods.

Table 2. Letter codes representing surface treatments on zirconia and test methods

	Group code	**Explanation**
Surface conditioning procedure	A	No further treatment following air abrasion, or air abrasion only
	U	After air abrasion, conditioning with Single Bond Universal according to the manufacturer's instructions
	Z	After air abrasion, conditioning with Z-Prime Plus according to the manufacturer's instructions
Bond strength test	F	Four-point flexural bond strength testing
	T	Tensile bond strength testing

2.3 Cementation of the resin cement to the zirconia

Experimental molds (inner dimensions 2 mm × 2 mm × 25 mm) were used as a matrix for cementation of the resin cement to the zirconia specimens. Surface-conditioned zirconia specimens were inserted into one side of the mold, with the treated surface facing towards the side of the resin cement being filled (**Fig. 2**). The composite resin cement (RelyX Ultimate, 3M ESPE) was mixed according to the manufacturer's instructions and filled into a single-dose plastic cap. Using the dispenser, the resin cement was inserted into the mold and covered with a cover-glass. The resin cement was light-cured for 60 s using a light-emitting diode curing device with a light intensity of 1,200 mW/cm^2 (Elipar FreeLight 2, 3M ESPE). The tip of the light unit was positioned in contact with the cover glass surface during light curing. To make sure that all areas received adequate amounts of light, overlapping of the tip was required since the area that had to be light-cured was larger (2 mm × 12.5 mm) than the tip of the light (8 mm in diameter). After light curing, the specimens were gently removed from the mold and left undisturbed for an hour to complete self-curing. The excess resin cement around the bonded area of the cemented specimen was removed and polished under a microscope to maintain an equal cross-sectional bonded area of approximately 4 mm^2 for every specimen. **Fig. 3** depicts the design and dimension of the final specimen.

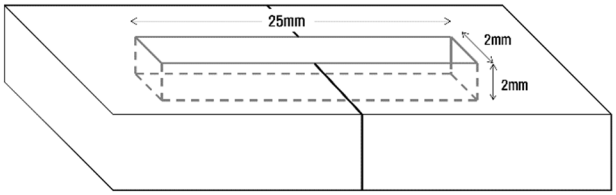

Fig. 2. Design and inner dimensions of the mold used for cementation of the zirconia specimens and resin cement. The mold could be separated, enabling the bonded specimen to be removed from the mold.

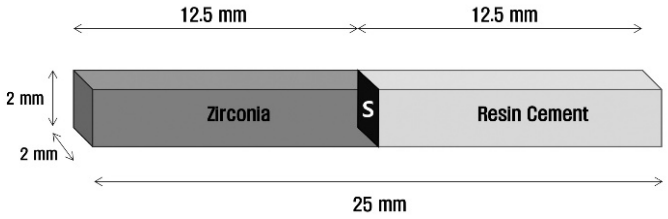

Fig. 3. Design and dimension of the final specimen. S, the bonded surface treated with three different surface treatment methods.

2.4 Experimental groups

The specimens of each surface treatment group (n = 60) were stored in a chamber at 37°C and 100% humidity for 24 h. After storage, each group was further divided randomly into two subgroups (n = 30) according to the two test

methods, with the four-point FBS test represented by the letter F and the TBS test represented by the letter T (see **Table 2** for the letter codes). Therefore, the group name 'FA' stands for specimens subjected to the FBS test (F) of the A group, and so forth (see **Table 3** for all group names and their explanations). The study design is schematically explained in **Fig. 4**.

Table 3. Experimental groups and their designations

Group	Explanation
FA	FBS test of the specimens conditioned with air abrasion only
FU	FBS test of the specimens conditioned with Single Bond Universal after air abrasion
FZ	FBS test of the specimens conditioned with Z-Prime Plus after air abrasion
TA	TBS test of the specimens conditioned with air abrasion only
TU	TBS test of the specimens conditioned with Single Bond Universal
TZ	TBS test of the specimens conditioned with Z-Prime Plus

Abbreviations: FBS, flexural bond strength; TBS, tensile bond strength

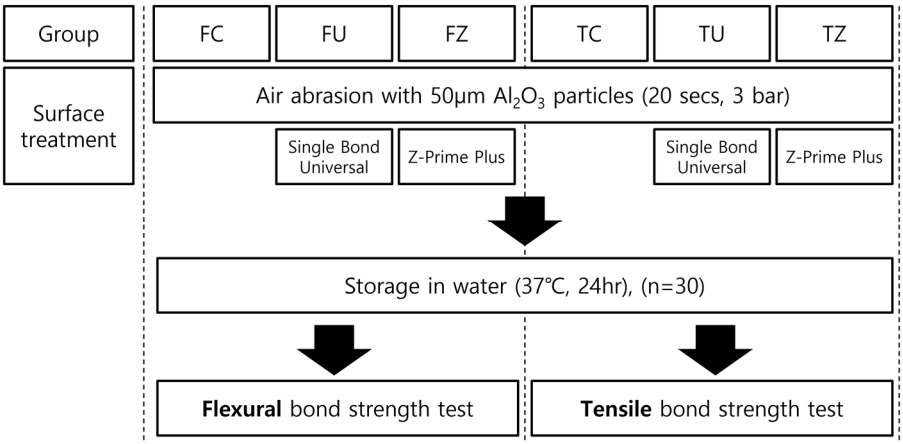

Fig. 4. Flow chart of the experimental design. Two different test methods: F, flexural bond strength test; T, tensile bond strength test. Three different surface conditioning procedures: A, air abrasion only group (no further treatment after air abrasion); U, conditioning with Single Bond Universal after air abrasion; Z, conditioning with Z-Prime Plus after air abrasion.

2.5 Four-point FBS test

The dimension of the adhesion interface was measured for each specimen using a digital calliper before performing the bond strength test. Final specimens of 25 mm in length were placed centrally between four rollers (span of loading rollers = 10 mm, span of supporting rollers = 20 mm) and were subsequently loaded until fracture with a crosshead speed of 0.5 mm/min in a

universal testing machine (LF Plus; Lloyd Instruments, Fareham, UK). **Fig. 5** depicts the test configuration. The force at break (N) was recorded and converted to MPa.

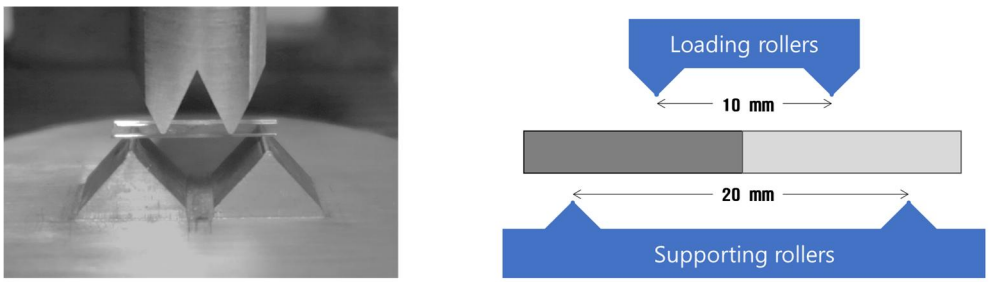

Fig. 5. Configuration and depiction on the four-point flexural bond strength test. The specimens were placed on two supporting pins a set distance apart and two loading pins located at an equal distance around the center. The distance between the loading pins was 10 mm and the distance between the supporting pins was 20 mm.

2.6 TBS test

Each side of the final specimens was mounted using a cyanoacrylate adhesive (Loctite 401; Henkel AG & Co, Düsseldorf, Germany) to a custom-made testing jig (**Fig. 6**) and loaded at a crosshead speed of 0.5 mm/min in a

universal testing machine until failure. The force at break (N) was recorded and converted to MPa.

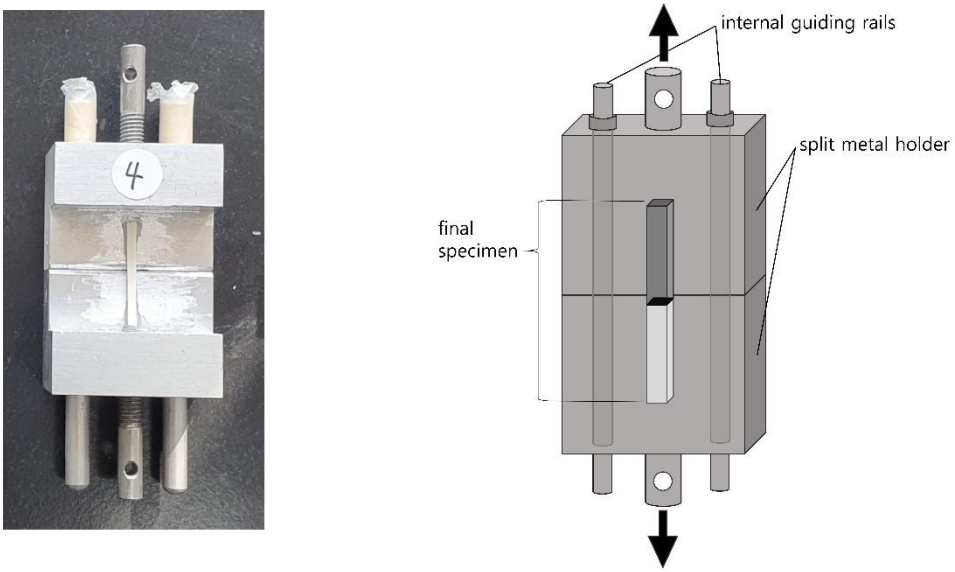

Fig. 6. Design of the custom-made testing jig for tensile bond strength test.

2.7 Data selection according to the failure mode

After the bond strength tests, the fractured surfaces were examined visually using a stereo-microscope (SZ-PT; Olympus, Tokyo, Japan) at a magnification 100x to determine whether the obtained values can be added in the data according to the failure modes. Data obtained from specimens showing cohesive failures were excluded from the analysis. The values obtained from those specimens showing mixed failures, which presented

partial cohesive fracture of resin cement concomitantly with adhesive failure, were included in the data.

2.8 Statistical analysis

In order to investigate the validity of the FBS test as an alternative to the TBS and MTBS test, the data were first evaluated using two-way ANOVA for surface treatment methods and test methods at a significance level of $\alpha = 0.05$, after conducting a Shapiro-Wilk test for normality. Second, the qualitative similarity between the FBS values and the TBS values and trends in the order of the bond strength values were also compared by fitting the data with two-parameter Weibull distributions. The parameters were estimated using the maximum likelihood estimation method, which takes the following form.

$$P_f = 1 - \exp(-(\sigma/\sigma_\theta\ )^m)$$

, where σ_θ is the scale parameter or characteristic strength and is dependent on the stress configuration and test specimen size, and m is the shape parameter (also referred to as the Weibull modulus). Third, according to Leguillon et al. (2015), the Weibull method can provide valuable insights when comparing flexural and tensile strengths. The quantitative relationship

between the FBS and TBS was simulated by theoretically calculating the ratio of the two strengths suggested by Leguillon et al. (2015). The ratios from the experimental results acquired from the above statistical analysis were compared with the theoretical ratios. According to Fard et al. (2014), the ratio R_{PB} between the flexural strength σ_C^{PB} and the tensile strength σ_C^T for four-point bending (4PB) can be derived as follows.

$$R_{4PB} = (\sigma_C^{4PB})/(\sigma_C^T\ ) = [(6(m+1)^2)/(m+3)]^{1/m}$$

, where m is the Weibull modulus used to calculate σ_C^{4PB} in the paper by Leguillon et al. (2015). Thereby, in this study, comparisons were made using three statistical approaches (ANOVA, Weibull fitting, and comparison of the experimental and theoretical ratios) to support the validity of the FBS test as an alternative to the TBS and MTBS tests.

2.9 Finite Element Analysis (FEA) for specimen experiments

An FEA was carried out to confirm the validity of the FBS test as an alternative to the TBS test, in addition to the three statistical verification steps. The objective of FEA was to explore the stress distribution over the specimens and

especially in the adhesive area. The specimen was modelled with eight-node solid elements (Fig. 7).

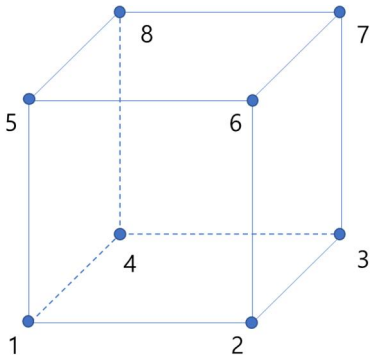

Fig. 7. A typical eight-node solid element.

First, the normal or axial stress distribution under tension and bending tests was analysed in FEA. Since the experiments are supposed to apply pure tension and bending, only small shear stresses that results from the differences of the Poisson's coefficient among different materials is observed from FEA. The stress components that we are discussing here depend on the coordinate systems we determine. For this reason, when we predict the yield strength of a material under complex loading, we should define and calculate stresses that are independent of a coordinate system, for example, von Mises stress and the maximum principal stress.

The von Mises stress is calculated as a scalar, which is then compared with the yield strength of the material. In terms of Cauchy stress tensor, it can be written as following:

$$\sigma_{\text{von Mises}} = \sqrt{\frac{1}{2}\left\{\left(\sigma_{xx} - \sigma_y\right)^2 + \left(\sigma_{yy} - \sigma_{zz}\right)^2 + (\sigma_{zz} - \sigma_{xx})^2\right\} + 3\left(\sigma_{yz}^2 + \sigma_{zx}^2 + \sigma_{xy}^2\right)}$$

Principal stresses are the corresponding normal stresses at a certain angle, where the shear stresses are zero. The maximum principal stress theory states that a material failure will occur if the maximum principal stress exceeds the ultimate strength of the material in case of a brittle material.

These stresses, von Mises stress and the maximum principal stress, are also obtained in FEA. However, since the axial stress component will be dominant, their results are similar to the normal stress σ_{33}. Therefore, we will compare the normal stress only, except for the case 1 of the tensile test, where all the stress results including normal stress, shear stress, von Mises stress, and the maximum principal stress will be shown.

Fig. 8 illustrates the specimen that consists of three parts, that is, composed of two materials and an adhesive in between. The dimension is 2 mm x 2 mm x 25 mm.

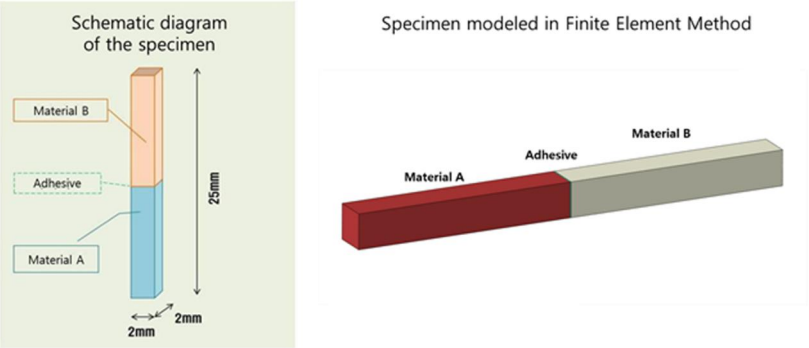

Fig. 8. Illustration of the basic numerical specimen. The specimen consists of three parts, which was composed of two materials and an adhesive in between.

The TBS and FBS tests were analysed respectively for a total of 14 cases consisting of different combinations of materials and the presence or absence of an adhesive. Materials that are used for 'Material A' part are zirconia, enamel, dentin, feldspathic porcelain, leucite, and lithium-di-silicate. Materials that are used for 'Material B' part are resin cement and composite resin, as shown in **Table 4.** The values of elastic moduli and Poisson's ratios for enamel and dentin (Dejak et al., 2008), feldspathic porcelain (Coelho et al., 2009), leucite (Yamanel et al., 2009), lithium-di-silicate (Lakshmi et al., 2015), zirconia (Silva et al., 2012), dental adhesive (Placido et al., 2007), resin cement (Asmussen et al., 2005) and composite resin (Chung et al., 2004; Jin et al., 2016) are listed in **Table 5**. The elastic modulus and Poisson's ratios were based on values that can be found in the literature.

Table 4. Cases of FEA with different materials and adhesive methods

	Material A	Adhesive	Material B
1	Zirconia	None	Resin cement
2	Zirconia	Adhesive	Resin cement
3	Enamel	None	Resin cement
4	Enamel	Adhesive	Resin cement
5	Dentin	None	Resin cement
6	Dentin	Adhesive	Resin cement
7	Feldspathic porcelain	None	Resin cement
8	Feldspathic porcelain	Adhesive	Resin cement
9	Leucite	None	Resin cement
10	Leucite	Adhesive	Resin cement
11	Lithium-di-silicate	None	Resin cement
12	Lithium-di-silicate	Adhesive	Resin cement
13	Enamel	Adhesive	Composite resin
14	Dentin	Adhesive	Composite resin

Table 5. Material properties of components used in the FEA models

	Elastic modulus (GPa)	Poisson ratio
Enamel	72.7	0.33
Dentin	18.6	0.31
Feldspathic porcelain	70	0.19
Leucite	67.2	0.3
Lithium-di-silicate	95	0.23
Zirconia	210	0.23
Dental adhesive	4	0.35
Resin cement	8	0.33
Composite resin	14	0.31

ABAQUS, a software suite for finite element analysis, was used in the analysis. The employed element was C3D8R, an 8-node solid element that is known to be useful for brittle materials. Total numbers of nodes are 57,771 and 58,653 for tensile and flexural tests, respectively, and total numbers of elements are 52,000 and 52,800 for tensile and flexural tests, respectively. As shown in **Fig. 9** and **Fig. 10**, z-axis was set for the axial or longitudinal direction. Thus, $S_{33} = S_{zz} = \sigma_{zz}$ = normal or tensile stress in the axial direction, and $S_{23} = S_{yz} = \sigma_{yz}$ = shear stress in the cross section.

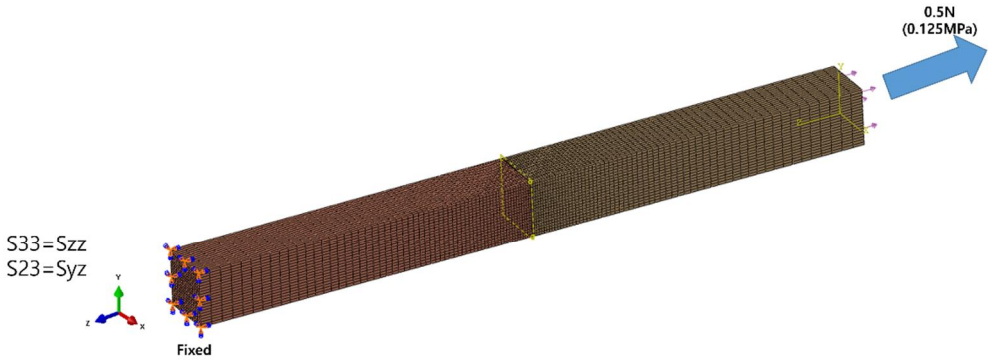

Total number of nodes	Total number of elements	Element type
57771	52000	C3D8R

Fig. 9. Modelling of tensile test. Tensile test was set up by fixing one end and pulling the other end as it was implemented in this experiment. Eight-node-solid element type was selected in the analysis (C3D8R).

For the tensile test shown in **Fig. 9**, a fixed boundary condition is applied at the left end as same as the tensile experiments. An external force is applied at the right end. For the flexural test shown in **Fig. 10**, a fixed boundary condition is applied at the location of supporting pins. An external force is applied at the loading pins as same as the experiments.

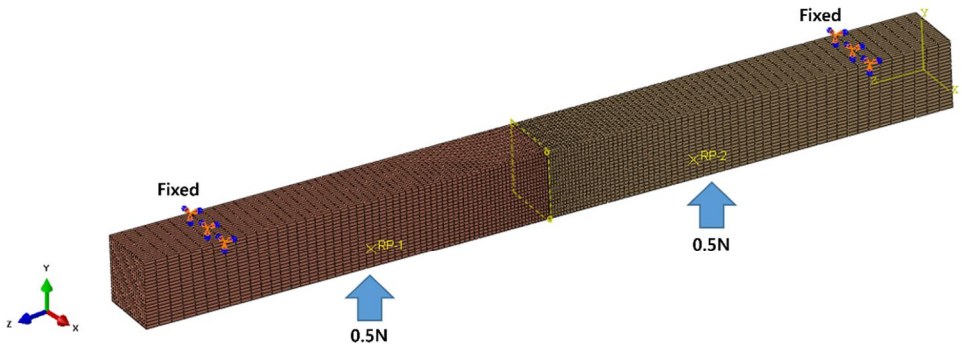

Total number of nodes	Total number of elements	Element type
58653	52800	C3D8R

Fig. 10. Modelling of 4-point flexural test. Flexural test was set up as a four-point bending by setting the locations of loading pins and supporting pins, as it was implemented in the experiment. The figure is rotated upside down to easily show the area under tension.

Chapter 3. Results

3.1 Statistical comparisons of TBS and FBS measurements

From the experimental data, descriptive statistics are tabulated in **Table 6** and two-way ANOVA results are shown in **Table 7**. The normality of residuals was met by the Shapiro-Wilk test ($p = 0.168$). In both FBS and TBS tests, the strength distributions of the A group (FA and TA) were the lowest among the three surface treatment groups. The strength values of the Z group (FZ and TZ) were higher than those of the A group, and the strength values of the U group (FU and TU) were the highest ($p < 0.0001$) (**Table 6** and **7**). The orders of the strength values were identical in both tests: A < Z < U. Both the experimental tests gave quite consistent results. For all three groups, the TBS values were lower than the FBS values ($p < 0.0001$) (**Table 6** and **7**). Although there was also an interaction effect between the two variables of test and surface treatment ($p < 0.0001$) (**Table 6** and **7**), the two line graphs of the FBS and TBS values according to the three surface treatments did not intersect; this can be confirmed by graphing the mean values shown in **Table 6**, and means that both test methods showed the same quantitative orders for the three surface treatments.

Table 6. Descriptive statistics of the flexural bond strength and tensile bond strength (MPa) of the three surface treatment groups

Test	**Flexural test**			**Tensile test**		
Group	FA	FU	FZ	TA	TU	TZ
Number of specimens (n)	28	29	29	28	26	26
Bond strength	13.2 ± 2.5	30.5 ± 3.4	20.3 ± 2.9	6.8 ± 1.8	17.5 ± 1.9	12.8 ± 1.5
Coefficient of variation (CV)	0.192	0.110	0.144	0.260	0.107	0.120
Ratio of CV_F to CV_T	0.738	1.028	1.200			

Values are shown as mean ± standard deviation. Abbreviations: CV, coefficient of variance; F, flexural bond strength test; T, tensile bond strength test; A, air abrasion only group (no further treatment after air abrasion); U, conditioning with Single Bond Universal after air abrasion; Z, conditioning with Z-Prime Plus after air abrasion; CV_F, CV of the flexural bond strength test; CV_T, CV of the tensile bond strength test.

Table 7. Two-way ANOVA table

	Df	**Sum Sq**	**Mean Sq**	**F value**	**Pr (>F)**	**Significance code†**
Surface	2	5692	2846	554.97	$< 2e^{-16}$	***
Test	1	3371	3371	657.26	$< 2e^{-16}$	***
Surface:Test	2	353	177	34.43	$3.45e^{-13}$	***
Residuals	162	831	5			

†Significance codes: '***', $p < 0.001$

The calculated coefficient of variance (CV) of the three surface treatment groups subjected to the FBS and TBS tests were in a relatively narrow range of 11% to 26%, showing quite acceptable results (**Table 6**). The ratio of the CV of the FBS test (CV_F) to the CV of the TBS test (CV_T) ranged from 0.7 to 1.2, indicating that the bond strength values measured by the FBS and TBS tests were scattered similarly according to the experimental surface treatment groups.

Table 8. Weibull parameters estimated by the maximum likelihood estimation method

Group	Number of specimens	Weibull modulus m	90% Confidence limits for m		Characteristic strength σ_θ, MPa	90% Confidence limits for σ_θ, MPa	
			Lower	Upper		Lower	Upper
FA	28	6.076	4.638	7.515	14.2	13.4	15.0
FZ	29	8.258	6.338	10.177	21.6	20.7	22.4
FU	29	10.988	8.394	13.582	32.0	31.0	32.9
TA	28	4.347	3.353	5.340	7.5	6.9	8.1
TZ	26	9.991	7.670	12.311	13.5	13.0	13.9
TU	26	11.281	8.585	13.977	18.3	17.8	18.9

F, flexural bond strength test; T, tensile bond strength test; A, air abrasion only group (no further treatment after air abrasion); U, conditioning with Single Bond Universal after air abrasion; Z, conditioning with Z-Prime Plus after air abrasion

The experimental data were then fitted with a Weibull distribution. **Table 8** shows the estimated parameters for all six groups by the maximum likelihood estimation method. The number of specimens in each group was less than that of the originally prepared 30 specimens, since the specimens with cohesive failures were excluded from the data. For each group, the distributions of the adhesive and mixed failures were as follow; 26 and 2 for FA, 18 and 11 for FZ, 20 and 9 for FU, 4 and 24 for TA, 3 and 23 for TZ, 6 and 20 for TU, respectively. **Fig. 11.** and **Fig. 12.,** as shown below, compares the Weibull distribution of the FBS and TBS test results, respectively, for the three surface treatment groups. The same pattern was found as in the results of the two-way ANOVA, in that the strength of the A group was the lowest among the three surface treatment groups, the strength of the Z group was higher than that of the A group, and the strength of the U group was the highest in both the FBS and TBS tests. The order of strengths in both tests (A < Z < U) was also identical to that obtained using ANOVA. Furthermore, comparisons of strength between the FBS and the TBS tests for each surface treatment group (graphs not shown) indicated that the TBS was lower than the FBS.

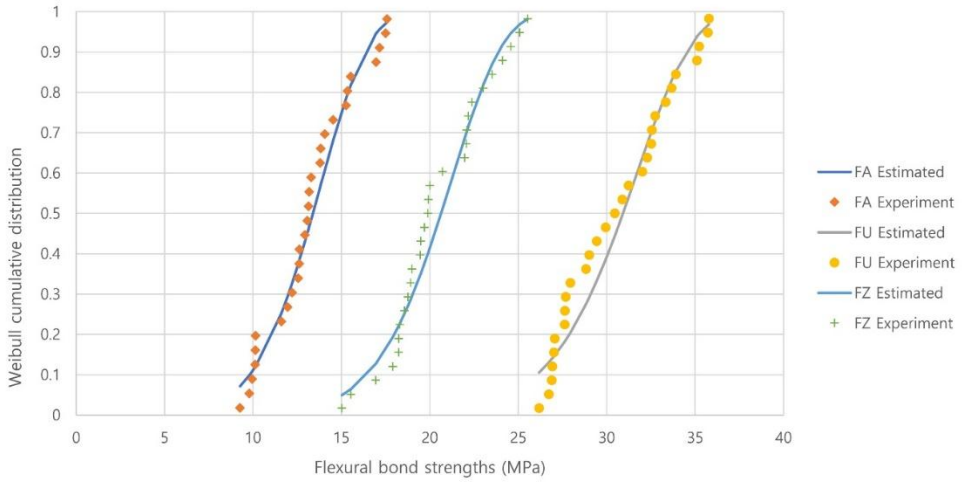

Fig. 11. Estimated Weibull cumulative distributions of the flexural bond strength test results using the 4-point bending test for three different surface treatment groups. Parameters for the Weibull distributions were estimated by the maximum likelihood estimation method.

For the three types of surface treatment methods, the ratios of the mean FBS values to the mean TBS values were calculated from the experimental results. The theoretical ratios, adopted from Leguillon et al. (2015) and from equation (2) in the paper by Fard et al. (2014), were calculated using the Weibull moduli in **Table 8**. The quantitative relationship of the theoretical and experimental ratios between the FBS values and TBS values were compared (**Table 9**). Although the ratios between the theoretical and experimental values were slightly different in each surface treatment group, all the ratios between

the FBS and the TBS values were greater than 1.0. This finding also means that the FBS was consistently greater than the TBS. Within the limitations of this study, the differences between the theoretical and experimental ratios in each group were relatively small, in the range of 0% to 16.5%.

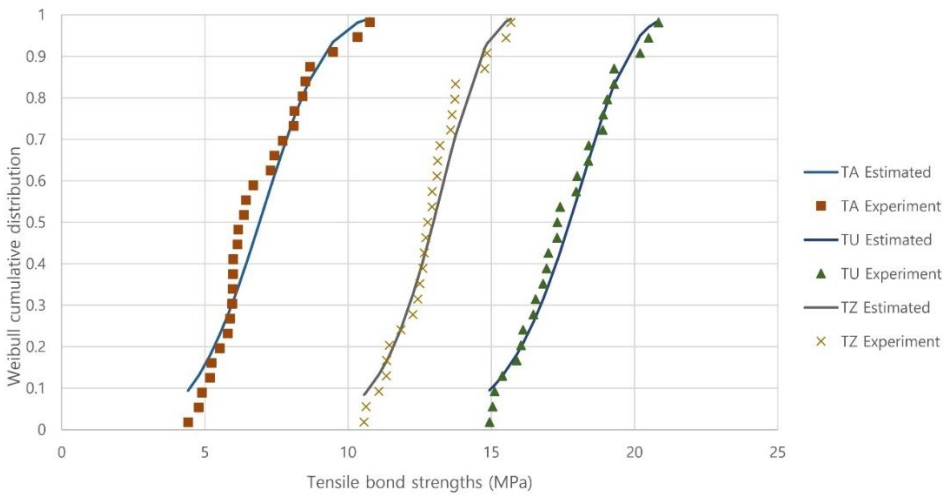

Fig. 12. Estimated Weibull cumulative distributions of the tensile bond strength test results for three different surface treatment groups. Parameters for the Weibull distributions were estimated by the maximum likelihood estimation method.

Table 9. Comparison of theoretical and experimental ratios between the mean bond strength values obtained by the flexural and tensile bond strength tests

	Air abrasion only (A)	**Single Bond Universal (U)**	**Z-Prime Plus (Z)**
Theoretical ratio ($\mathbf{R_{4PB}}$)	1.779 (m = 6.076)	1.455 (m = 10.988)	1.589 (m = 8.258)
Experimental ratio	1.927	1.743	1.589
Theory/Experiment	0.923 (7.7% difference)	0.835 (16.5% difference)	0.999 (0.001% difference)

Abbreviations: R_{4PB}, the ratio R_{PB} between the flexural σ_C^{PB} and tensile σ_C^T strengths for four-point bending (4PB).

3.2 FEM analysis

Fig. 13 and **Fig. 14** are representative figures of the FEM analysis for tensile test and four point bending test. It is not intended to exhibit a specific case, but to give an overall explanation. For both **Fig. 13** and **Fig. 14**, the top image shows the specimen model in whole. The middle image shows the divided specimen to reveal the junctional surface. The top and middle image display change in color due to the automatic alteration of the numerical range, however, the stress magnitude itself is the same. The bottom image is a flipped over image of the divided halves to show the opposite rear end. The adhesive layer in the lower right corner only apears in cases with the use of an adhesive.

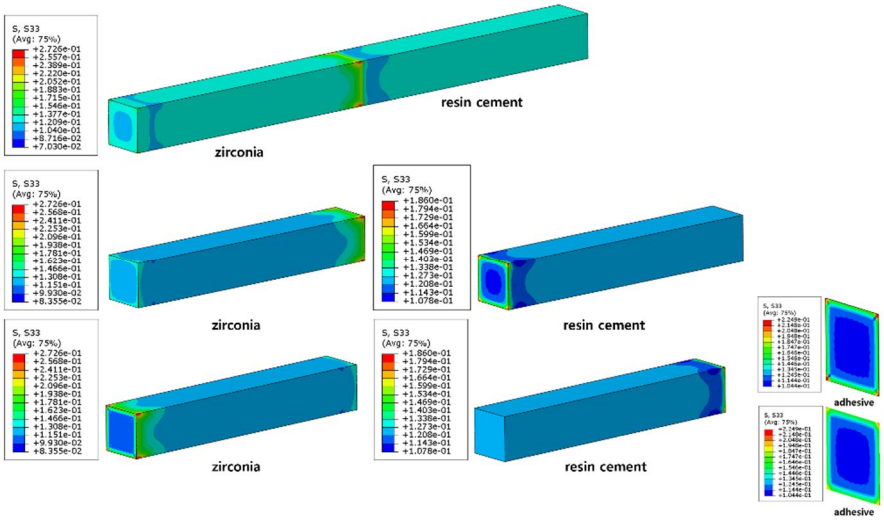

Fig. 13. Constitution of the figures showing the result of FEM analysis for tensile test modelling. The even distribution of color shows that the specimen was under pure tension. The color difference at the rear end of the zirconia results from the fact that it was fixed. The color difference near the bonding surface shows the change of stress distribution due to the difference in Poisson's ratio of the adjacent materials.

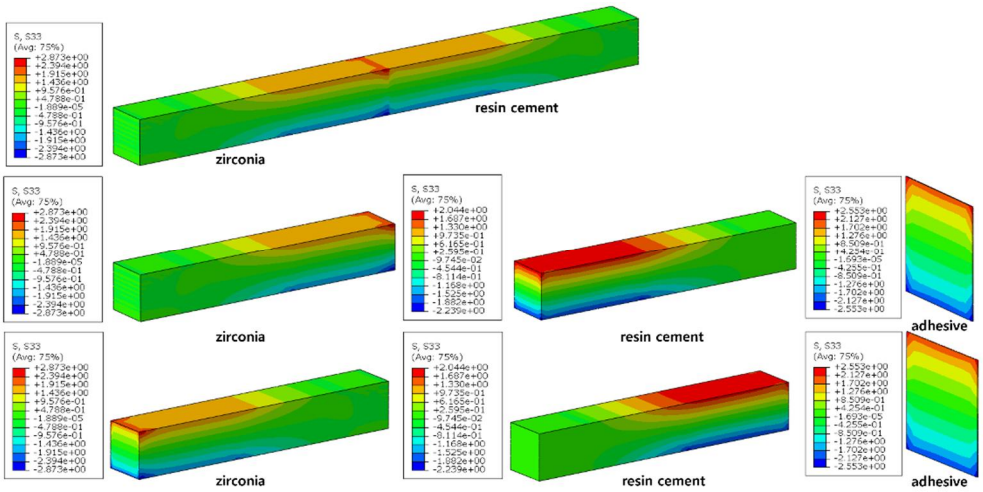

Fig. 14. Constitution of the figures showing the result of FEM analysis for 4-point flexural test modelling. The figures are shown upside down compared to the experimental model so that the stress distribution on the bottom can be visualized.

The results from FEA for case 1 are illustrated in **Fig. 15** ~ **Fig. 20**. This finite element analysis is intended to look at the overall trend. For case 1, the stress distributions in tensile and flexural tests are shown in two figures each: One for the normal stress S_{zz} and the other for the S_{yz} to compare the relative magnitude between them. In general, S_{yz} is much smaller when compared to S_{zz}. Therefore, S_{zz} is almost the same as the principal stress. Since this tendency is the same for all the other cases, S_{yz} is omitted for the rest of the cases. Tensile stress is constant except in the zone adjacent to the boundary

and adhesive. Tensile test for case 1 also includes two other figures: they are results for the von Mises stress and the maximum principal stress.

Fig. 15 shows the normal stress distribution under tension in Case 1. The order of magnitude ranges from 10^{-2} to 10^{-1}. **Fig. 16** shows the shear stress distribution under tension in Case 1. The order of magnitude ranges from 10^{-3} to 10^{-2}. It can be confirmed that the normal stress component is dominant. **Fig. 17** shows the von Mises stress in Case 1. Although the numbers are a bit different, the order of magnitude remains the same as the normal stress. **Fig. 18** shows the maximum principal stress in Case 1. Again, the order of magnitude remains the same as the normal stress and magnitude itself is very close to the normal stress. Therefore, for simplicity, the von Mises and the maximum principal stresses will not be provided from Case 2.

Fig. 19 shows the normal stress distribution under four-point bending in Case 1 and **Fig. 20** shows the shear stress distribution under four-point bending in Case 1. For the four-point bending cases, the figures are shown upside down, so that the stress distribution on the bottom can be seen. Just like the tensile test, flexural test results also showed that the normal stress is much higher than the shear stress. Therefore, the normal stress component is the most important stress component. The complete results of the tests can be found in the appendix.

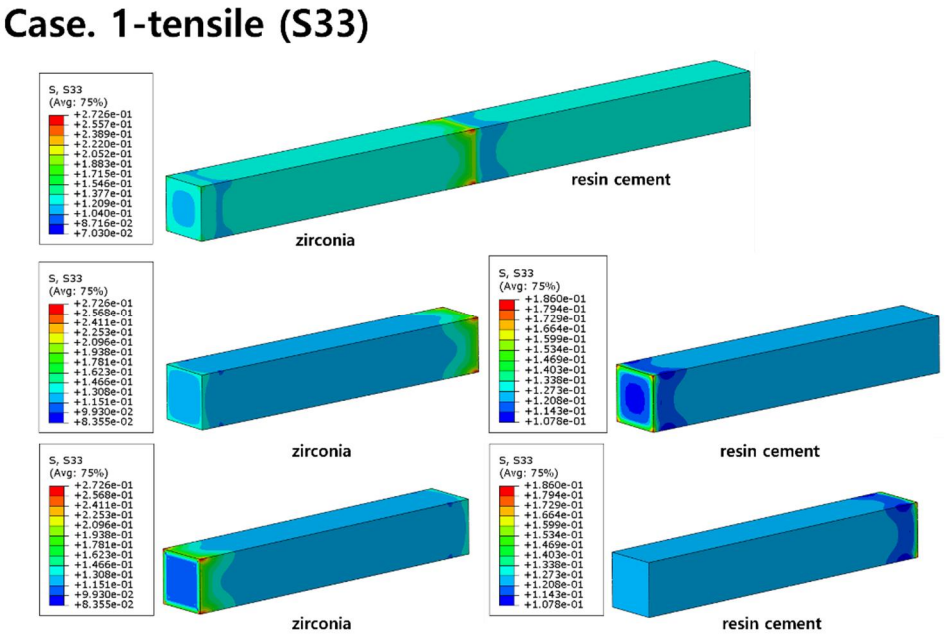

Fig. 15. Normal stress distribution under tension in Case 1.

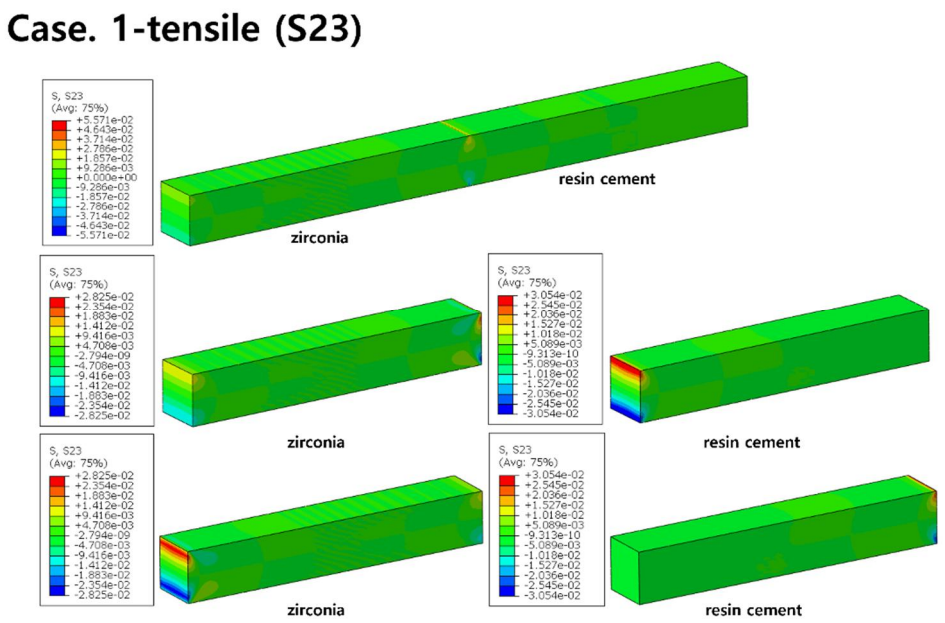

Fig. 16. Shear stress distribution under tension in Case 1.

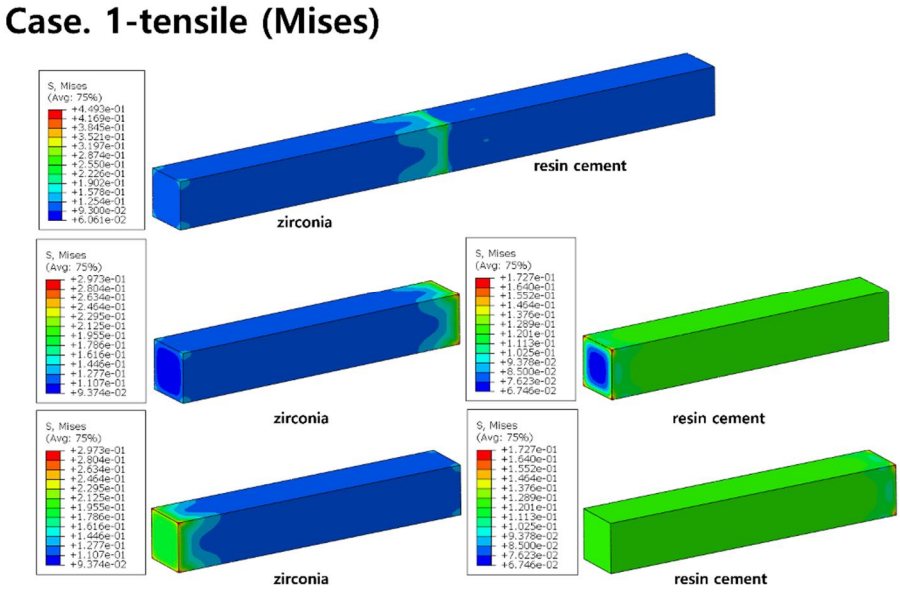

Fig. 17. Von Mises stress distribution under tension in Case 1.

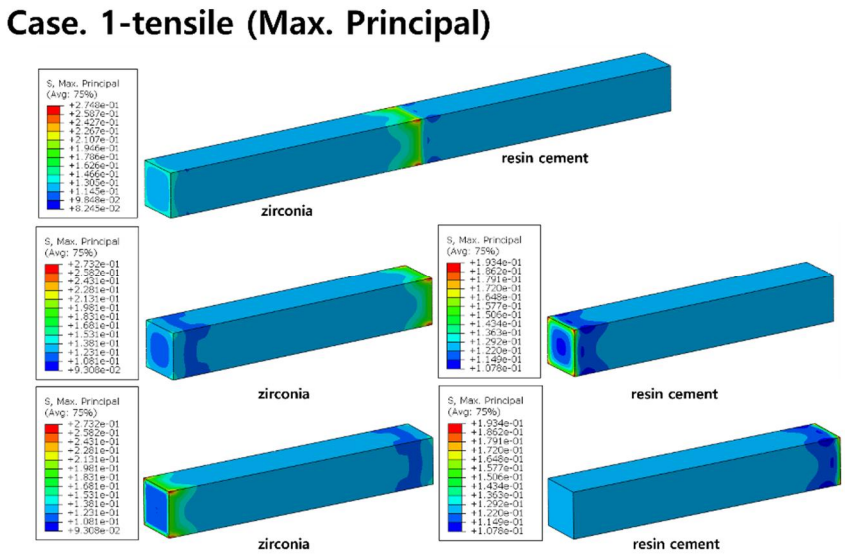

Fig. 18. Maximum Principal stress distribution under tension in Case 1.

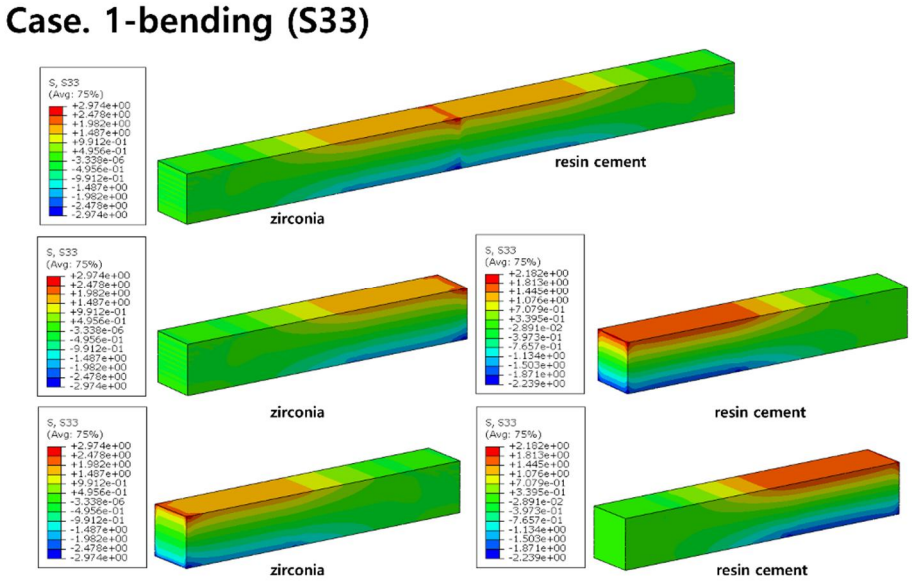

Fig. 19. Normal stress distribution under 4-point bending in Case 1.

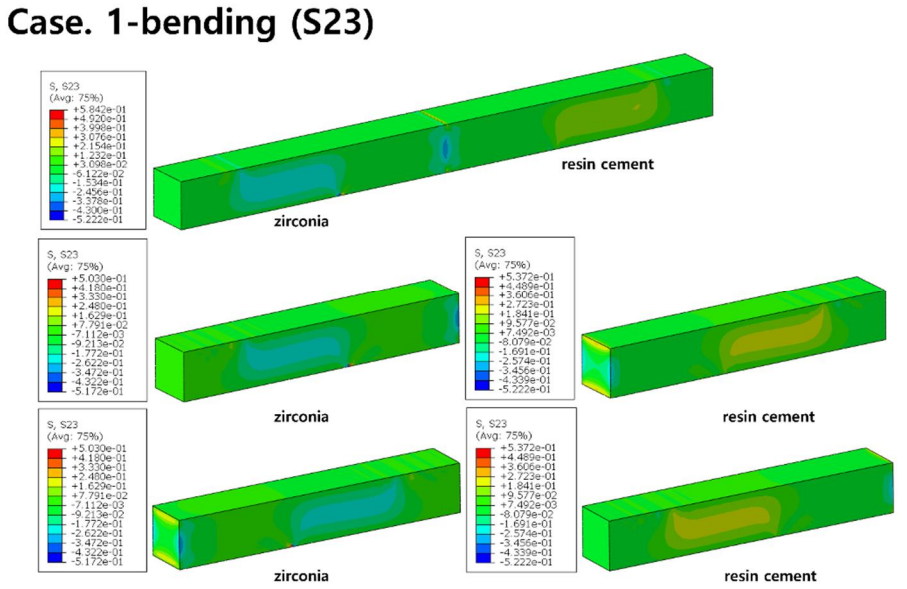

Fig. 20. Shear stress distribution under 4-point bending in Case 1.

The finite element analysis showed that the maximum stress occurred at the same region of the specimen for both test methods, namely, adjacent to the bonded region. The maximum stress occurs near the surface of the bonded region in the virtual models of both tests (**Fig. 15** and **Fig. 19)**. This observation in the case 1 was also observed for all the 14 cases.

Since the normal stress component was still dominant compared to the shear stress, the specimen would fail due to the tensile stress. When a specimen is loaded in an FBS test, the bottom bonded region was under tension (**Fig. 19**). Therefore, in both tests, the specimen will fail when the maximum tensile stress exceeds a certain limit, such as ultimate tensile strength.

For those cases with adhesive layer (**Fig. 21** and **Fig. 22**), the maximum stress mostly occurs between the Zirconia and the adhesive layer, while for those cases without adhesive layer, the maximum occurs between the zirconia and resin cement. In either case, the maximum stress occurs at the center region of the specimen, the bonded area, regardless of whether it is the TBS or the FBS test. In other words, the failure mechanisms of both tests are basically the same, whether there is an adhesive layer or not, and similar stress distribution patterns can be observed.

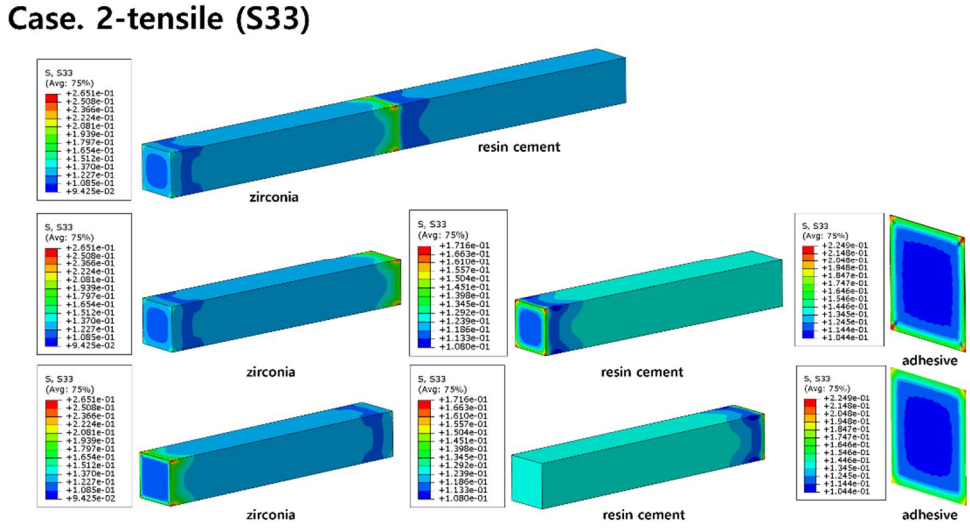

Fig. 21. Normal stress distribution under tension in Case 2.

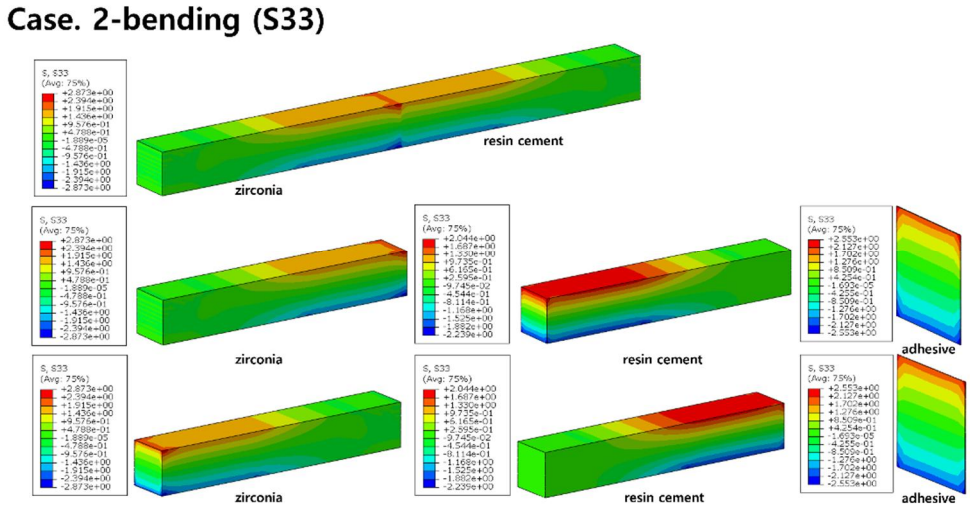

Fig. 22. Normal stress distribution under 4-point bending in Case 2.

Chapter 4. Discussion

In the clinical dentistry, the bond strength values have been widely used as a relatively easy and fast method to compare the performance of new dental materials (Bouillaguet et al., 2003; Münchow et al., 2013). However, the test protocols for the TBS and MTBS tests are quite complicated for evaluating the bond strength of dental adhesives and resin cements to brittle substrates (Sano et al., 1994; Pashley et al., 1995). The specimen preparation and equipment setup such as specimen alignment and mounting of specimen on the jig make it vulnerable to error, which results in high variability of test data (Pashley et al., 1995). In case of the MTBS test, the testing specimens need to be cut from bonded samples. Because of the brittle characteristics of the dental adhesion and substrate materials, preparing (cutting and grooving) the test specimens and measuring their bond strengths (aligning the specimen on the testing jig) for the MTBS test in adhesive dentistry requires very difficult and labor-intensive procedures (Ferrari et al., 2002; Pashley et al., 1995). Cutting and measuring procedures should be performed after 24 hours from bonding to minimize specimen loss by immediate cutting of the bonded samples. In addition, there are variations in data sets among bonded samples or teeth (inter-sample variations) even within the same group. Furthermore, in spite of the TBS test being a preference for measuring interfacial bond strength, no

wide agreement has been reached in standardizing the method (Sano et al., 1994; Silva et al., 2006; Van Noort et al., 1989; Van Noort et al., 1991). Thus, it is difficult to be used or to compare the results among various researchers.

In contrast, the FBS test is widely used to test brittle materials (Leguillon et al., 2015) and is relatively easy to carry out. The purpose of this study was to confirm the validity of the FBS test as an easier alternative to the commonly accepted TBS and MTBS tests in adhesive dentistry, especially for analyzing brittle dental adhesion. To this end, the adhesion of resin cement to zirconia, which is widely used as an aesthetic restorative material, was examined using the FBS and TBS tests. The possibility of the FBS test as a more convenient alternative experimental method that can replace the TBS test was confirmed by obtaining consistent results through three statistical verification steps: quantitative comparison of experimental FBS and TBS values between surface treatment groups using conventional ANOVA, verification of the qualitative similarity using Weibull fitting with the ANOVA results, and a comparison of the ratios between the mean experimental FBS and TBS values and the theoretical ratios. In addition, using a finite element analysis, the validity of the FBS test as an alternative to the TBS was verified again by comparing the stress distribution within the virtual

models of the specimens in both test configurations. A similar pattern in stress distributions within both the virtual models were also confirmed.

First, the normality of residuals was met by the Shapiro-Wilk test ($p = 0.168$) and two-way ANOVA was carried out. From the experimental data for the two variables of test method (FBS and TBS tests) and surface treatment (air abrasion only, conditioning with Single Bond Universal after air abrasion, and conditioning with Z-Prime Plus after air abrasion), the mean bond strength values were significantly different in the order of A < Z < U within each test method ($p < 0.0001$). In all the surface treatment groups, the FBS test yielded significantly higher mean bond strength values than the TBS test ($p < 0.0001$). As for the interaction effect between the two variables of test method and surface treatment, the line graphs of the FBS and TBS values according to the three surface treatments did not intersect, which means that both test methods showed the same quantitative orders for the three surface treatments. In this experiment, definite discrimination of the mean bond strength values was observed among the surface treatment groups and between the test methods. In this study, the regression equation is not discussed since all the variables, which are test methods and surface treatment methods, are categorical. Instead, the orders of the bond strength values were frankly compared within each variable.

Second, the validity of the FBS test as an alternative to the TBS test was assessed using Weibull statistics. The Weibull distribution is widely used for the statistical analysis of failure data from brittle materials (Weibull, 1939; Weibull, 1951). Assuming that the flaws of various sizes have a normal distribution, the largest flaws are associated with the smallest strength values (i.e., the flaws which are the weakest link in the material). The distribution of the largest flaws is referred to as an extreme value distribution. According to QUINN & QUINN (2010), the Weibull distribution is usually considered the best choice among the extreme value distributions. Thus, the Weibull distribution was adopted in this paper to evaluate the qualitative similarity between the FBS values and the TBS values. Since a qualitative similarity among subgroups under the same condition exists, the FBS test can be suggested as an alternative to the TBS test. The estimated Weibull parameters of the experimental groups by 2 test methods were calculated by the maximum likelihood estimation method, because the test results followed the estimated Weibull distributions quite well. **Fig. 11.** and **Fig. 12.** depict the Weibull distributions of the FBS and TBS test results, respectively, for the three surface treatment groups. In both the FBS and TBS tests, the bond strength distributions were the same as those in the ANOVA; that is, the order of strengths were identical in both tests (A < Z < U). When comparisons between

the FBS and TBS tests were made for each surface treatment as a Weibull cumulative distribution (graphs not shown), the TBS was confirmed to be lower than the FBS in all the surface treatment groups. Therefore, the results of the Weibull statistics aligned quite well with those of ANOVA.

As the third verification process, a theoretical simulation of the ratio of the stress caused by the flexural test to that caused by the tensile test was compared with the ratio of the mean strength values obtained experimentally by the FBS test to those by the TBS test. Many efforts have been made to identify a quantitative relationship between the tensile and flexural strength tests. Leguillon et al. (2015) compared flexural and tensile strength in brittle materials. Bhushan et al. (2016) derived semi-analytical expressions for effective volume and effective surface for a cylindrical bar loaded in flexure, and calculated the strength scaling ratio between two different loading configurations Fard et al. (2014), described the ratio R_{PB} between the flexural σ_C^{PB} and tensile σ_C^T strengths for four-point bending (4PB) in equation (2). The theoretical ratio between the FBS and TBS given by equation (2) is shown in **Table 9**. Note that the Weibull modulus, *m*, used in this equation was estimated using experimental data. In material technical sheets provided by manufacturers, knowing the flexural strength, the tensile strength is sometimes derived using the ratio without new measurements,

since bending experiments are easier to carry out for brittle materials (Leguillon et al., 2015). As is shown in **Table 9**, for the A group, the theoretical and experimental ratio values differed by about 7.7%, for the U group, by 16.5%, and for the Z group, by 0.001%. Therefore, the theoretical and experimental ratios showed some differences for the A and U groups but gave almost identical values for the Z group in this study. All the ratios of the experimental mean values of the FBS and TBS were greater than 1.0, which means the FBS values were consistently greater than the TBS values, as stated earlier. Within the limitations of this study, the differences between the theoretical and experimental ratios in each group were relatively small, in the range of 0% to 16.5%.

As the fourth verification process, the finite element analysis was carried out to analyse and compare the stress distributions under TBS and FBS. The observation in the finite element analysis that the maximum stress occurred at the same region of the specimen for both test methods, namely, adjacent to the bonded region, implies that the specimen would fail at the same region when loaded with bending as it would when it is loaded with tension. Furthermore, it was shown that the maximum stress occurs near the surface of the bonded region in the virtual models of both tests (**Fig. 15** and **Fig. 19)**. This observation can be confirmed not only for the case 1, but also for all the

14 cases. The two loading conditions may seem very different. However, they work exactly in the same fashion when we look at the bonded region.

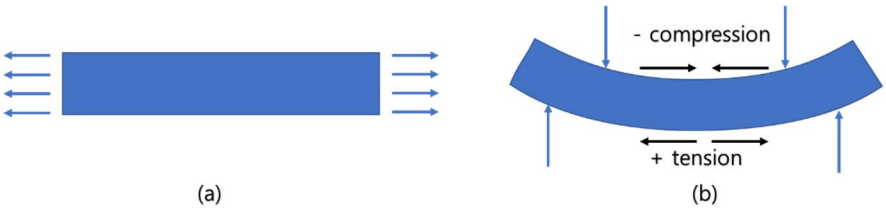

Fig. 23. Specimen under tension (a) and specimen under bending (b)

When a specimen is loaded in a TBS test (**Fig. 23(a)**), it is under nearly uniaxial tension. It would be under uniform tension if the material was homogeneous. Due to the material inhomogeneity, there would be slight disturbance. However, according to the FEA observation, since the normal stress component was still dominant, the specimen would fail due to the tensile stress. When a specimen is loaded in FBS test, although the loading pins in the four-point bending test are applied in a perpendicular direction, the bottom bonded region in **Fig. 23(b)** is under tension. The specimen would fail due to the tensile stress, just the same way it would in a TBS test. In both tests, the specimen will fail when the maximum tensile stress exceeds a certain limit, which may be the ultimate tensile strength of the adhesive layer (Dickens and Cho, 2005). Hence, the two tests essentially have the same mechanism of

failure; therefore, the flexural bond strength test can consider to be an alternative to the tensile bond strength test.

The FBS test can be performed by three-point bending or four-point bending. In a three-point bending test, the loading point overlaps with the adhesive joint (i.e., the maximum stress point). Because of the stress concentration at the adhesive joint, it might be difficult to measure the strength precisely. However, in the four-point bending test, the loading point does not overlap with the adhesive joint since the adhesive joint is placed in-between the symmetric plunging rollers. Therefore, four-point bending test results in measuring the strength precisely and consistently; this study utilized a four-point bending test. Also, since it is more likely to place the tensile stress at the bottom of the centrally placed adhesive joint, the specimens from the FBS test presented more adhesive failures than those from TBS test.

If an object undergoing the four-point bending test was formed of a single material, there is no doubt that the peak stress is spread along the extended region of the specimen surface (**Fig. 23(b)).** On the other hand, if the object being loaded had various components and the parts located under the two loading pins were not equal as in our present study, one might query the constant stress between the two loading points. According to the FEA observation, where the modelled specimen consists of three parts, two

materials and an adhesive in between, showed even and symmetrical stress distribution despite the different combination of materials (**Fig. 19** and **Fig. 22**).

The fracture strength values obtained from the specimens showing cohesive failures within the resin cement was discarded, since the cohesive failures present the strength of the resin cement itself and not the real bond strength of the resin cement to zirconia. Since the flexural strength and flexural modulus of RelyX ultimate were reported 134 MPa and 5.5 GPa and those of IPS e.max ZirCAD were 845 MPa and 210 GPa, respectively (Bacchi et al., 2014; Basso et al., 2015), these values far exceeded the expected adhesion values. It was predicted that the stress would be concentrated on the relatively weak adhesion interface. In fact, in our previous study, cohesive failures within the composite cylinders or zirconia were not observed even in MSBS test (Kim et al., 2015). Therefore, the specimens showing cohesive failure were considered as technical errors during packing of the resin cement into the mold as the other half against zirconia and excluded from the data. There were 10 cohesive failures for TBS specimens and 4 for FBS specimens.

In this study, the validity of the FBS test as an alternative to the TBS test is confirmed through three statistical verification steps and additional FEA comparisons. However, in the dental field, the MTBS test has been a standard

test method which can reduce the probability of inadvertent flaw distribution since the suggestion by Sano et al. (1994). Using the MTBS test, in which the bonded surface areas were reduced from 4 mm^2 (2 x 2 mm) to 1 mm^2 (1 x 1 mm), the adverse effect of inadvertent large population of flaws were excluded and, as a result, measured MTBS values were higher than those by TBS test. The MTBS test has definite advantages in dentin adhesion, such as small number of adherend substrates (extracted teeth) and intended bond strengths of small, selected areas. However, reducing the bonded surface in the MTBS test method also causes several inherent disadvantages, such as difficulties in specimen preparation and testing procedures, excessive loss of specimens, inability to obtain immediate bond strength values, and inter-sample variations (Ferrari et al., 2002; Goracci et al., 2004; Loguercio et al., 2005). In the dental field, further research is needed to evaluate if the FBS and MFBS tests to various dental materials can be an alternative to the TBS, MTBS, and MSBS tests through the comparison of bond strength, specimen loss, and changes in failure modes according to the surface area in adhesion.

Chapter 5. Conclusions

The experimental data in this study gave quite consistent results in three statistical analyses and additional FEA comparisons. First, according to two-way ANOVA, the experimental data of the FBS test and the TBS test were in the same order of strengths in both tests (FBS > TBS) and in all surface treatment groups (A < Z < U). Second, the findings were also confirmed by the Weibull fitting, which showed the same order of strengths in both tests (FBS > TBS) and in all surface treatment groups (A < Z < U). Third, the theoretical ratio calculated from the Weibull moduli quite closely agreed with the experimental ratio of the FBS to the TBS. In addition, using a finite element analysis (FEA), it was verified again by observing a similar pattern in stress distributions within the virtual models of the specimens in both test configurations. Based on the results of these three statistical analyses and FEA, it can be concluded that the four-point bending FBS test can be used as an alternative to the TBS, MTBS tests to compare the performance of dental adhesives in experimental conditions.

Acknowledgements – A part of this thesis has been published in the Journal of the Mechanical Behavior of Biomedical Materials. This work was supported by the Ministry of Trade, Industry & Energy of Republic of Korea under the Technology Innovation Program (10052089, Technology-leading Open Platform for Dental Instrumentation). Author sincerely thanks Prof. Jong Gye Shin and Dr. Youngmin Kim at Seoul National University for their valuable discussions on material strength and statistics, respectively, and Prof. Yuil Kim at Inha University for his support of finite element analysis.

Disclosure of interest – The author reports no conflict of interest.

Bibliography

Afferrante, L., Ciavarella, M., Valenza, E., 2006. Is Weibull's modulus really a material constant? Example case with interacting collinear cracks. Int. J. Solds Struct. 43, 5147-5157.

Al-Zain, A., Marghalani, H., 2020. Influence of Light-curing Distances on Microflexural Strength of Two Resin-based Composites. Oper. Dent. 45, 297-305.

Armstrong, S., Breschi, L., Özcan, M., Pfefferkorn, F., Ferrari, M., Van Meerbeek, B., 2017. Academy of Dental Materials guidance on in vitro testing of dental composite bonding effectiveness to dentin/enamel using micro-tensile bond strength (μTBS) approach. Dent. Mater. 33, 133-143.

Asmussen, E., Peutzfeldt, A., & Sahafi, A., 2005. Finite element analysis of stresses in endodontically treated, dowel-restored teeth. J. Prosthet. Dent. 94(4), 321-329.

Attia, A., Lehmann, F., & Kern, M., 2011. Influence of surface conditioning and cleaning methods on resin bonding to zirconia ceramic. Dent. Mater. 27(3), 207-213.

Bacchi, A., Dobson, A., Ferracane, J., Consani, R., Pfeifer, C., 2014. Thio-urethanes improve properties of dual-cured composite cements. J. Dent. Res. 93, 1320-1325.

Basso, G., Moraes, R., Borba, M., Griggs, J., Della Bona, A., 2015. Flexural strength and reliability of monolithic and trilayer ceramic structures obtained by the CAD-on technique. Dent. Mater. 31, 1453-1459.

Bermejo, R., Danzer, R., 2014. Mechanical characterization of ceramics: designing with brittle materials. Comprehensive Hard Materials. 2, 285-298.

Bhushan, A., Panda, S., Khan, D., Ojha, A., Chattopadhyay, K., Kushwaha, H., Khan, I., 2016. Weibull effective volumes, surfaces, and strength scaling for cylindrical flexure specimens having bi-modularity. J. Test. Eval. 44, 1978-1997.

Bouillaguet, S., Troesch, S., Wataha, J. C., Krejci, I., Meyer, J.-M., Pashley, D. H., 2003. Microtensile bond strength between adhesive cements and root canal dentin. Dent. Mater. 19, 199-205.

Chung, S. M., Yap, A. U. J., Koh, W. K., Tsai, K. T., & Lim, C. T. (2004). Measurement of Poisson's ratio of dental composite restorative materials. Biomaterials. 25(13), 2455-2460

Coelho, P. G., Bonfante, E. A., Silva, N. R. F., Rekow, E. D., & Thompson, V. P.. 2009. Laboratory simulation of Y-TZP all-ceramic crown clinical failures. J. Dent. Res., 88(4), 382-386.

Dejak, B., & Mlotkowski, A.. 2008. Three-dimensional finite element analysis of strength and adhesion of composite resin versus ceramic inlays in molars. J. Prosthet. Dent., 99(2), 131-140.
Dickens, S. H., Cho, B. H., 2005. Interpretation of bond failure through conversion and residual solvent measurements and Weibull analyses of flexural and microtensile bond strengths of bonding agents. Dent. Mater. 21, 354-364.
Dobi, D., Junghans, E., 1999. Determination of the tensile properties of specimens with small dimensions. Kovine Zlitine Tehnologije(Slovenia) 33, 451-457.
El Zohairy, A. A., Saber, M. H., Abdalla, A. I., Feilzer, A. J., 2010. Efficacy of microtensile versus microshear bond testing for evaluation of bond strength of dental adhesive systems to enamel. Dent. Mater. 26, 848-854.
Eshmawi, Y. T., Al-Zain, A. O., Eckert, G. J., Platt, J. A., 2018. Variation in composite degree of conversion and microflexural strength for different curing lights and surface locations. J. Am. Dent. Assoc. 149, 893-902.
Fard, M. Y., Raji, B., Chattopadhyay, A., 2014. The ratio of flexural strength to uniaxial tensile strength in bulk epoxy resin polymeric materials. Polym. Test. 40, 156-162.
Ferrari, M., Goracci, C., Sadek, F., Cardoso, P. E. C., 2002. Microtensile bond strength tests: scanning electron microscopy evaluation of sample integrity before testing. Eur. J. Oral Sci. 110, 385-391.
Fornazari, I. A., Brum, R. T., Rached, R. N., de Souza, E. M., 2020. Reliability and correlation between microshear and microtensile bond strength tests of composite repairs. J. Mech. Behav. Biomed. Mater. 103, 103607.
Ghassemieh, E., 2008. Evaluation of sources of uncertainties in microtensile bond strength of dental adhesive system for different specimen geometries. Dent. Mater. 24, 536-547.
Gianola, D. S., Eberl, C., 2009. Micro-and nanoscale tensile testing of materials. JOM. 61, 24-35.
Goracci, C., Tavares, A. U., Fabianelli, A., Monticelli, F., Raffaelli, O., Cardoso, P. C., Tay, F., Ferrari, M., 2004. The adhesion between fiber posts and root canal walls: comparison between microtensile and push-out bond strength measurements. Eur. J. Oral Sci. 112, 353-361.
Inokoshi, M., Shimizubata, M., Nozaki, K., Takagaki, T., Yoshihara, K., Minakuchi, S., Vleugels, J., Van Meerbeek, B., Zhang, F., 2021. Impact of sandblasting on the flexural strength of highly translucent zirconia. J. Mech. Behav. Biomed. Mater. 115, 104268.

Inoue, S., Vargas, M. A., Abe, Y., Yoshida, Y., Lambrechts, P., Vanherle, G., Sano, H., Van Meerbeek, B., 2001. Microtensile bond strength of eleven contemporary adhesives to dentin. J. Adhes. Dent. 3, 237-245

Jin, X. Z., Homaei, E., Matinlinna, J. P., & Tsoi, J. K. H., 2016. A new concept and finite-element study on dental bond strength tests. Dent. Mater. 32(10), e238-e250.

Kim, J.-H., Chae, S., Lee, Y., Han, G.-J., Cho, B.-H., 2014. Comparison of shear test methods for evaluating the bond strength of resin cement to zirconia ceramic. Acta Odontol. Scand. 72, 745-752.

Kim, J., Chae, S., Lee, Y., Han, G., Cho, B., 2015. Effects of multipurpose, universal adhesives on resin bonding to zirconia ceramic. Oper. Dent. 40, 55-62.

Lakshmi, R. D., Abraham, A., Sekar, V., & Hariharan, A., 2015. Influence of connector dimensions on the stress distribution of monolithic zirconia and lithium-di-silicate inlay retained fixed dental prostheses–A 3D finite element analysis. Tanta Dent. J. 12(1), 56-64.

Laurencin, J., Delette, G., Dupeux, M., 2008. An estimation of ceramic fracture at singularities by a statistical approach. J. Eur. Ceram. 28, 1-13.

Leguillon, D., Martin, E., Lafarie-Frenot, M.-C., 2015. Flexural vs. tensile strength in brittle materials. CR. Mécanique. 343, 275-281.

Loguercio, A. D., Barroso, L. P., Grande, R., Reis, A., 2005. Comparison of intra-and intertooth resin-dentin bond strength variability. J. Adhes. Dent. 7, 151-158.

Münchow, E. A., Bossardi, M., Priebe, T. C., Valente, L. L., Zanchi, C. H., Ogliari, F. A., Piva, E., 2013. Microtensile versus microshear bond strength between dental adhesives and the dentin substrate. Int. J. Adhes. Adhes. 46, 95-99.

Nakamura, K., Adolfsson, E., Milleding, P., Kanno, T., Örtengren, U., 2012. Influence of grain size and veneer firing process on the flexural strength of zirconia ceramics. Eur. J. Oral Sci. 120, 249-254.

Pashley, D. H., Sano, H., Ciucchi, B., Yoshiyama, M., & Carvalho, R. M., 1995. Adhesion testing of dentin bonding agents: a review. Dent. Mater. 11(2), 117-125.

Placido, E., Meira, J. B., Lima, R. G., Muench, A., de Souza, R. M., & Ballester, R. Y., 2007. Shear versus micro-shear bond strength test: a finite element stress analysis. Dent. Mater. 23(9), 1086-1092.

Qeblawi, D. M., Muñoz, C. A., Brewer, J. D., & Monaco Jr, E. A., 2010. The effect of zirconia surface treatment on flexural strength and shear bond strength to a resin cement. J. Prosth. Dent. 103(4), 210-220.

Quinn, G. D., 2003. Weibull strength scaling for standardized rectangular flexure specimens. J. Am. Ceram. Soc. 86, 508-510.
Quinn, J. B., Quinn, G. D., 2010. A practical and systematic review of Weibull statistics for reporting strengths of dental materials. Dent. Mater. 26, 135-147.
Sano, H., Shono, T., Sonoda, H., Takatsu, T., Ciucchi, B., Carvalho, R., Pashley, D. H., 1994. Relationship between surface area for adhesion and tensile bond strength—evaluation of a micro-tensile bond test. Dent. Mater. 10, 236-240.
Shimada, Y., Yamaguchi, S., Tagami, J., 2002. Micro-shear bond strength of dual-cured resin cement to glass ceramics. Dent. Mater. 18, 380-388.
Silva, N. R., Bonfante, E., Rafferty, B. T., Zavanelli, R. A., Martins, L. L., Rekow, Coehlo, P. G., 2012. Conventional and modified veneered zirconia vs. metalloceramic: fatigue and finite element analysis. J. Prosthodont. 21(6), 433-439.
Silva, N. R., Calamia, C. S., Harsono, M., Carvalho, R. M., Pegoraro, L. F., Fernandes, C. A., Vieira, A. C., Thompson, V. P., 2006. Bond angle effects on microtensile bonds: laboratory and FEA comparison. Dent. Mater. 22, 314-324.
Thammajaruk, P., Inokoshi, M., Chong, S., Guazzato, M., 2018. Bonding of composite cements to zirconia: A systematic review and meta-analysis of in vitro studies. J. Mech. Behav. Biomed. Mater. 80, 258-268.
Van Noort, R., Noroozi, S., Howard, I., Cardew, G., 1989. A critique of bond strength measurements. J. Dent. 17, 61-67.
Van Noort, R., Cardew, G., Howard, I., Noroozi, S., 1991. The effect of local interfacial geometry on the measurement of the tensile bond strength to dentin. J. Dent. Res. 70, 889-893.
Versluis, A., Tantbirojn, D., Douglas, W. H., 1997. Why do shear bond tests pull out dentin? J. Dent. Res. 76, 1298-1307.
Visintini, E., Mazzoni, A., Vita, F., Pasquantonio, G., Cadenaro, M., Di Lenarda, R., Breschi, L., 2008. Effects of thermocycling and use of ElectroBond on microtensile strength and nanoleakage using commercial one-step self-etch adhesives. Eur. J. Oral Sci. 116, 564-570.
Weibull, W., 1939. A statistical theory of the strength of materials. Swed. R. Inst. Eng. Res. 151, 1-45.
Weibull, W., 1951. A statistical distribution function of wide applicability. J Appl Mech. 18, 290-293.
Yamanel, K., Çaglar, A., Gülsahi, K., & Özden, U. A., 2009. Effects of different ceramic and composite materials on stress distribution in inlay

and onlay cavities: 3-D finite element analysis. Dent. Mater. J., 28(6), 661-670.
Zhang, S., Kocjan, A., Lehmann, F., Kosmač, T., Kern, M., 2010. Influence of contamination on resin bond strength to nano-structured alumina-coated zirconia ceramic. Eur. J. Oral Sci. 118, 396-403.

국문초록

지르코니아 세라믹에 대한 레진 시멘트의 굽힘접착강도 시험을 통한 인장접착강도 시험에 대한 대안 연구: 통계 및 유한요소법적 해석

신 유 진

서울대학교 대학원

치의과학과 치과보존학 전공

(지도교수 조 병 훈)

1. 목 적

표면처리 방법에 따른 지르코니아 세라믹에 대한 레진 시멘트의 굽힘접착강도와 인장접착강도를 실험을 통하여 실험군 간의 접착강도의 차이와 그 경향을 비교하고 분석하여, 굽힘접착강도시험의 인장접착강도시험에 대한 대체 실험으로서의 가능성을 제시하였다.

.

2. 방 법

시편 제작 및 표면 처리와 접착

CAD/CAM용 지르코니아 블록 (IPS e.max ZirCAD)을 완전 소결하여 막대형 (2 mm x 2 mm x 12.5 mm) 지르코니아 시편을 준비하여 표면처

리 방법에 따라 세 실험군으로 분류하였다; 미세입자 분사마모 표면처리 (A), 미세입자 분사마모 표면처리 후 Single Bond Universal (3M ESPE) 적용 (U), 미세입자 분사마모 표면처리 후 Z-Prime Plus (BISCO) 적용 (Z). 표면처리한 지르코니아는 내면이 2 mm x 2 mm x 25 mm인 아크릴릭 몰드의 절반에 표면처리한 면이 레진시멘트와 접착될 수 있게 삽입하고, 몰드의 나머지 절반에는 레진 시멘트 (RelyX Ultimate)를 채워 최종적으로 지르코니아와 레진시멘트가 접착된 2 mm x 2 mm x 25mm인 시편을 제작하였다. 모든 시편은 온도 37℃, 습도 100%에서 24시간 보관하였다.

굽힘접착강도와 인장접착강도 측정 방법

제작된 시편을 2 가지 접착강도 측정 방법에 따라 하위군으로 나누었다; 굽힘접착강도 (F), 인장접착강도 (T). 굽힘접착강도시험은 4절점 굽힘시험방법을 채택하였다. 4절점 굽힘접착강도 시험은 내부 하중점의 간격은 10 mm, 외부 지지대의 간격은 20 mm로 하였다. 압축력을 가하여 시험편이 파절될 때의 최대 하중을 측정하였다. 인장접착강도는 시편을 실험용 지그에 고정하여 인장력을 가하고 파절될 때의 응력을 기록하였다.

데이터의 분석

3가지 표면처리 방법과 2가지 접착강도 측정 방법에 따라 얻어진 접착강도 값은 분산분석을 통한 정량적 분석과 Weibull 분포식을 이용하여 정성적인 비교를 수행하였다. 또한 2015년 Leguillon등이 취성 재료의 인

장강도와 굽힘강도 간의 수치관계를 수식으로 제시한 이론적 계산식을 활용해 실험적 비와 이론적 비를 비교하였다. 나아가 유한요소 분석법을 사용하여 편성된 가상 시편 내 응력 분포를 비교하여 실험 결과를 이용한 수치해석의 가능성을 확인해 보았다.

3. 결 과

굽힘접착강도와 인장접착강도 시험치는 정량적으로 유사하며 서로 일관된 경향을 보였다. 두 가지 접착강도 시험 모두에서 U그룹이 가장 높은 접착강도를 보였으며, Z 그룹, A 그룹 순으로 그 값은 낮아졌다 (p<0.001). 같은 표면처리를 한 시편 군 내에서는 굽힘접착강도가 인장접착강도 보다 항상 높은 수치를 나타냈다 (p<0.001). Weibull 분포식에서도 두 가지 접착강도 시험 모두 U>Z>A 순의 분포가 나타났으며 같은 표면처리를 한 경우 굽힘접착강도가 인장접착강도보다 큰 분포를 보였다 (p<0.001). Weibull 계수를 반영하여 계산한 이론적 비와 실험적 비 역시 유사한 경향을 보였다. 마지막으로 유한요소 분석법을 통해 가상 시편 내 응력분포 또한 유사한 패턴을 나타냄을 확인하였다.

4. 결 론

치과용 접착제의 성능을 비교함에 있어서 가장 널리 사용되지만 그 시험방법이 어렵고 복잡한 인장접착강도 측정법을 대신하여 시험 방법이 보다 안정적이고 단순한 굽힘접착강도 측정법의 사용 가능성을 접착강도 시험 값의 통계적 분석, Weibull 통계 분석, 이론적 계산식을 활용한 비

교 및 유한요소법으로 검증하였다.

주요어: 치과용 접착, 굽힘접착강도, 인장접착강도, 지르코니아 세라믹, 통계분석, 유한요소법적 분석
학번: 2014-30704

Appendix: Complete results of FEA

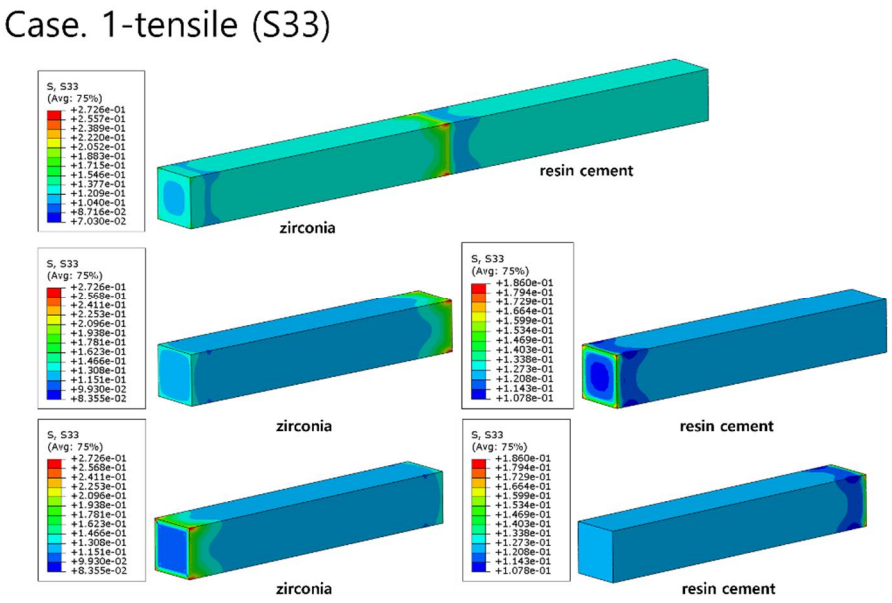

Fig. 24. Normal stress distribution under tension in Case 1

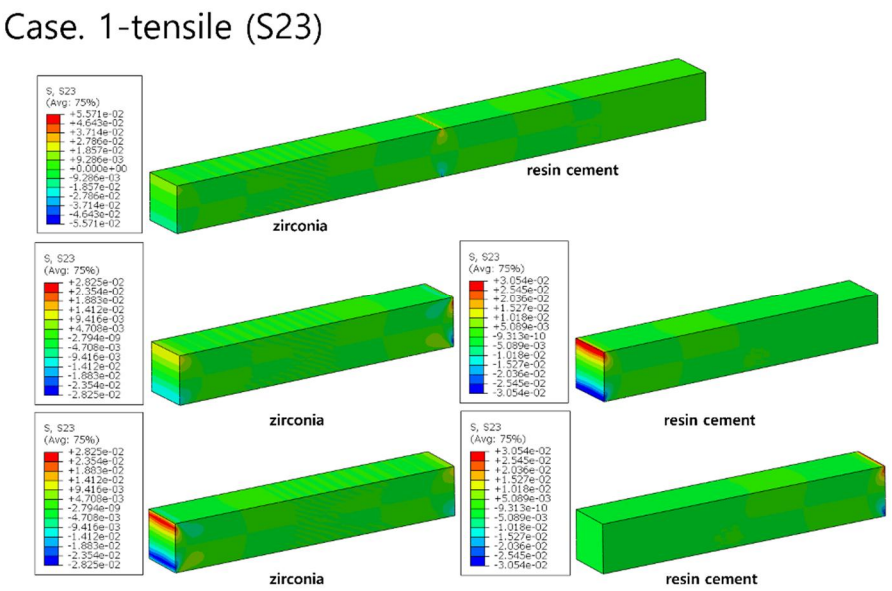

Fig. 25. Shear stress distribution under tension in Case 1

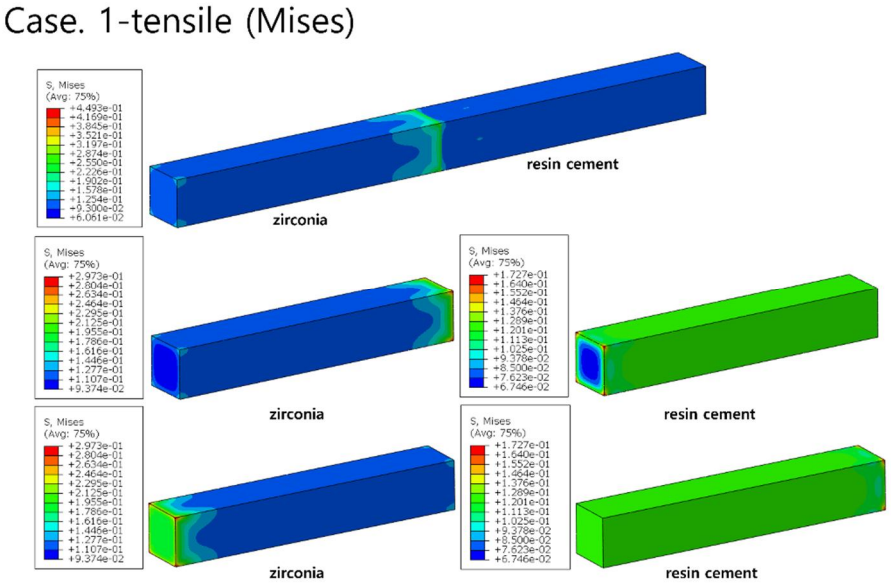

Fig. 26. Von Mises stress distribution under tension in Case 1

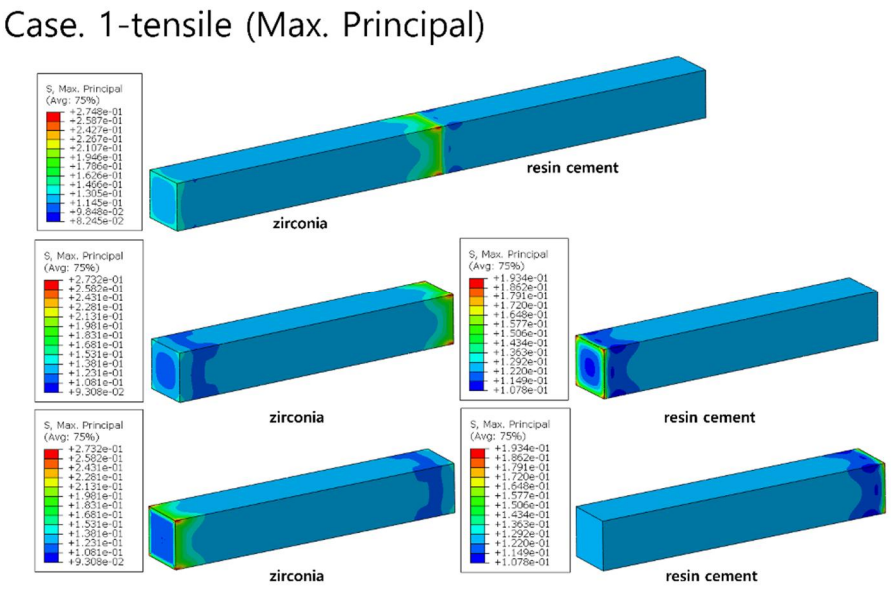

Fig. 27. Maximum Principal stress distribution under tension in Case 1

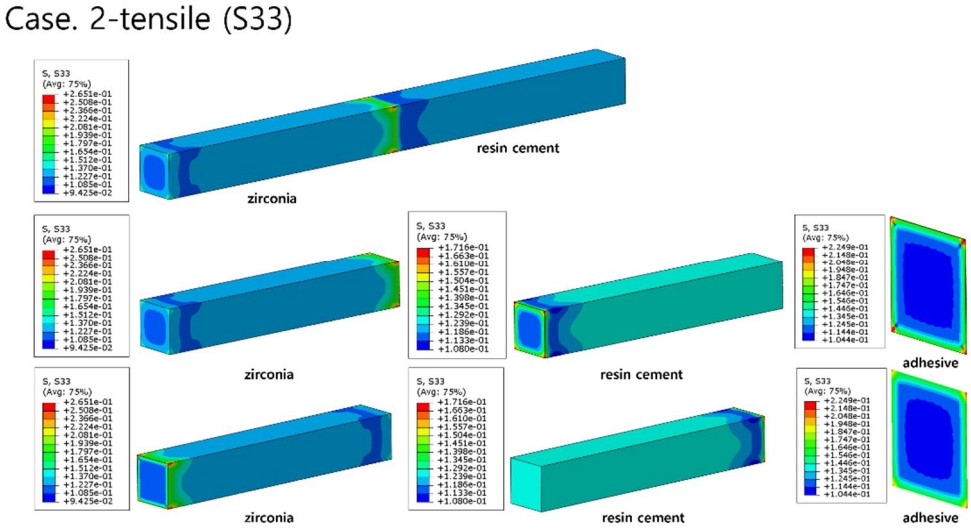

Fig. 28. Normal stress distribution under tension in Case 2

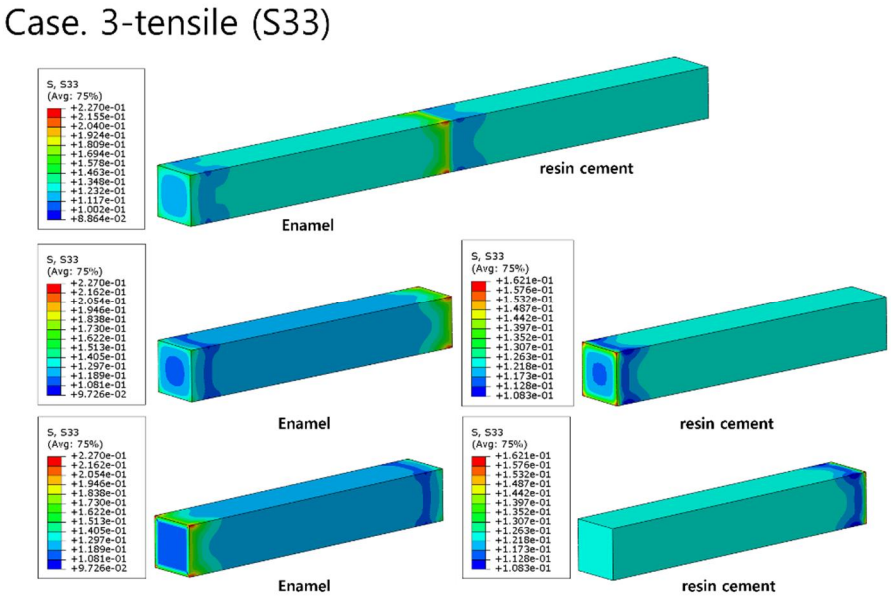

Fig. 29. Normal stress distribution under tension in Case 3

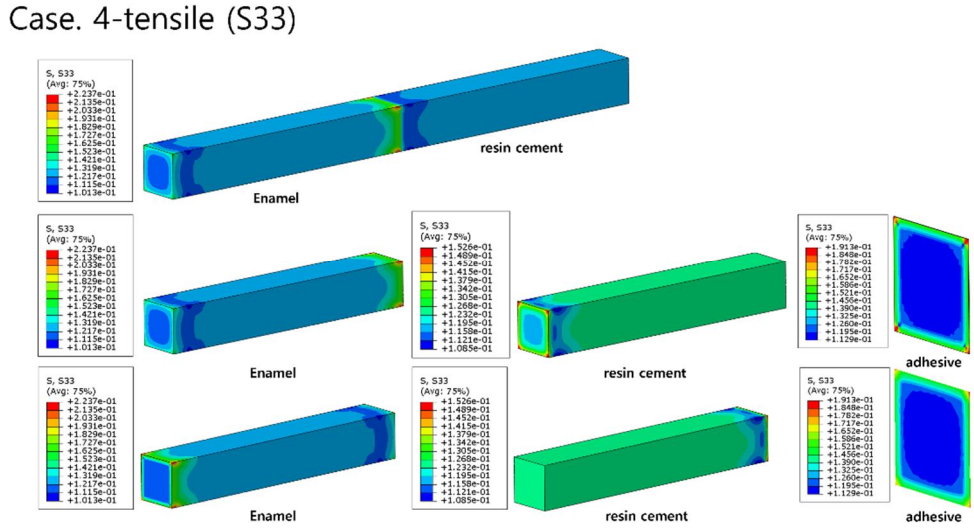

Fig. 30. Normal stress distribution under tension in Case 4

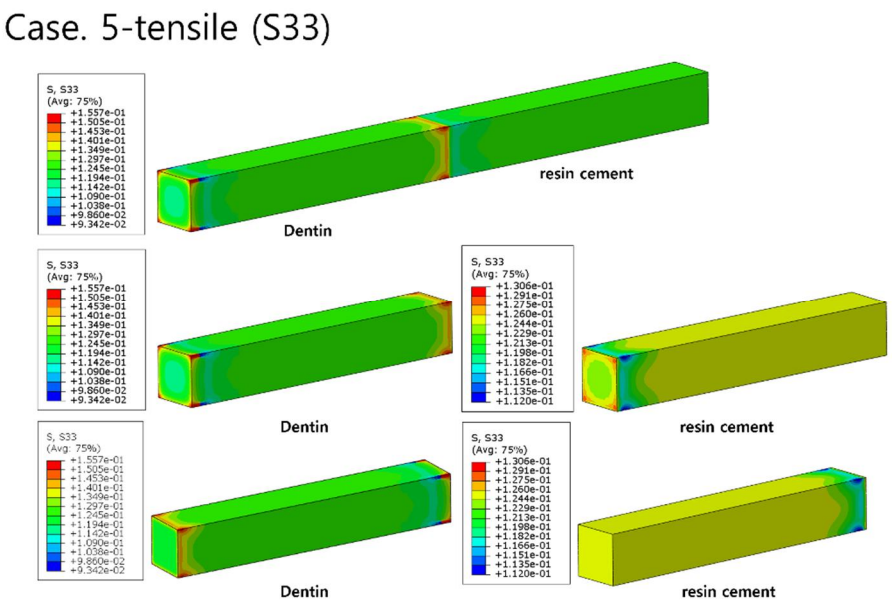

Fig. 31. Normal stress distribution under tension in Case 5

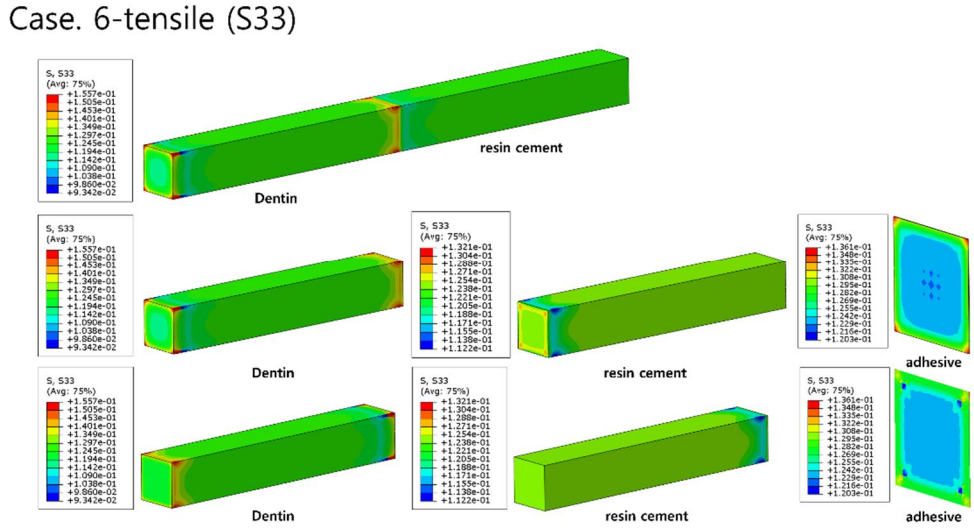

Fig. 32. Normal stress distribution under tension in Case 6

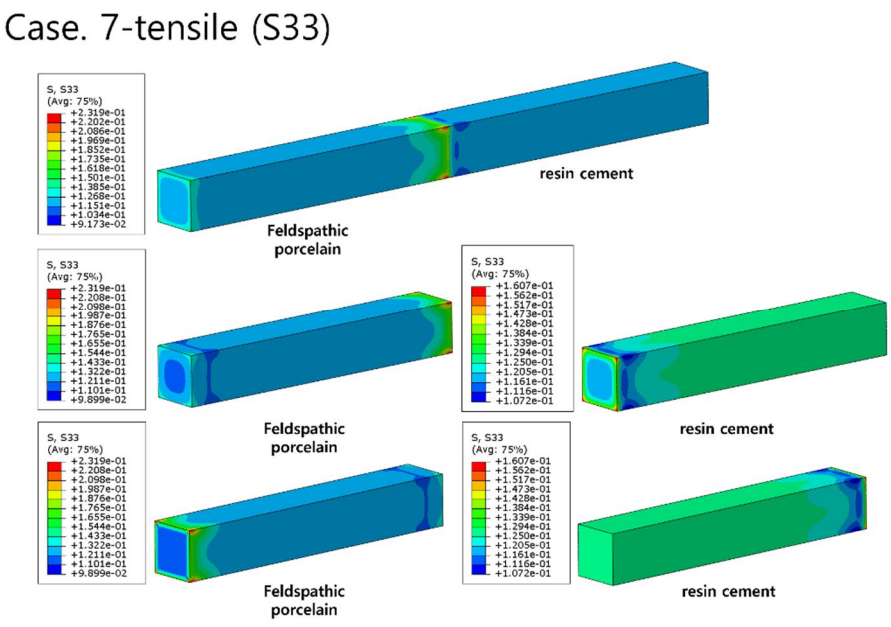

Fig. 33. Normal stress distribution under tension in Case 7

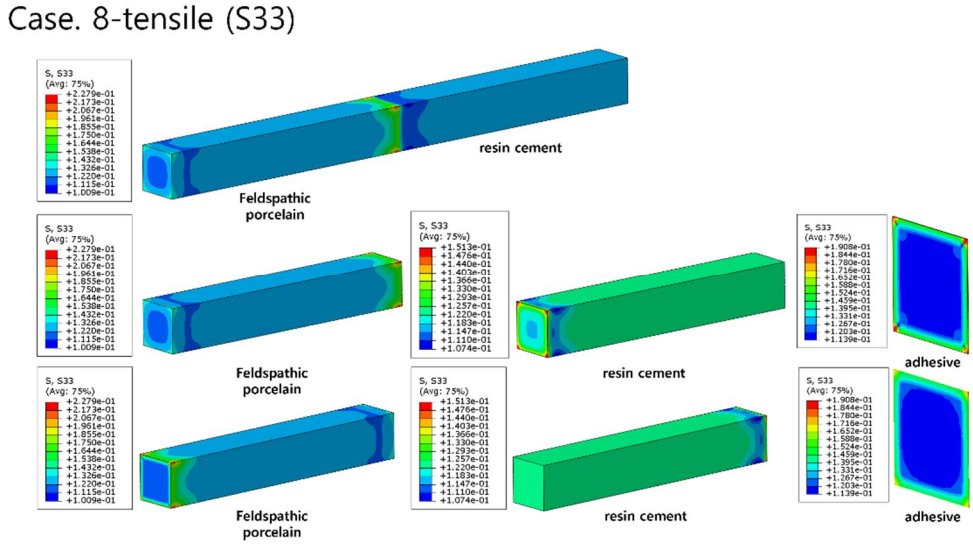

Fig. 34. Normal stress distribution under tension in Case 8

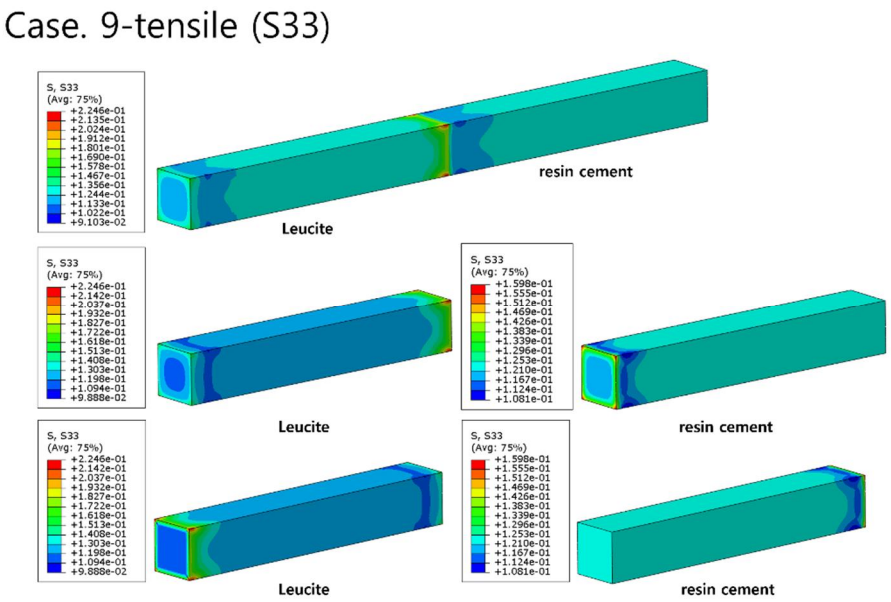

Fig. 35. Normal stress distribution under tension in Case 9

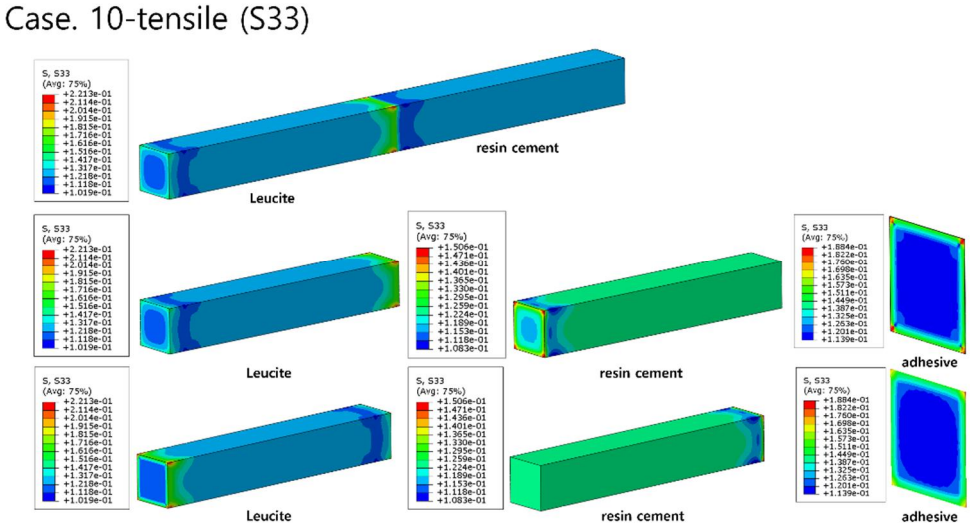

Fig. 36. Normal stress distribution under tension in Case 10

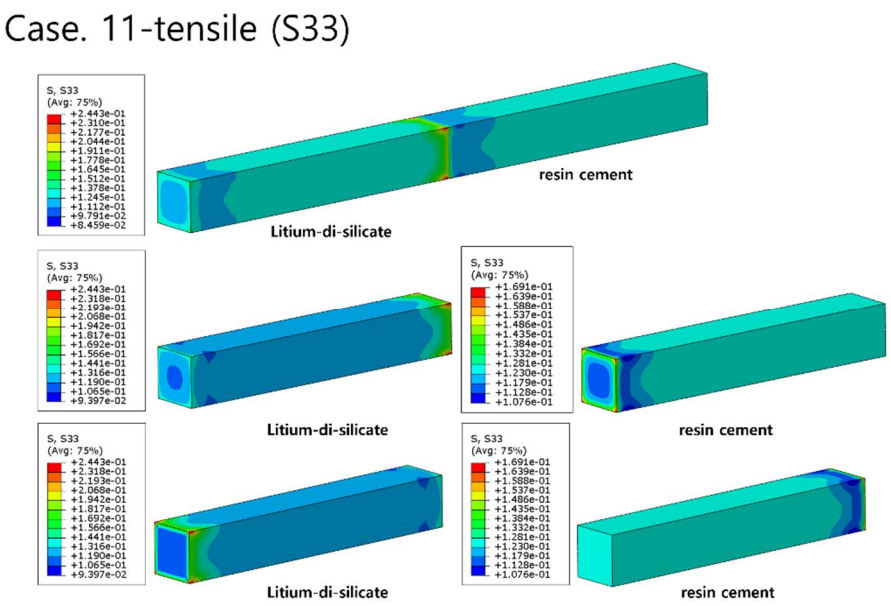

Fig. 37. Normal stress distribution under tension in Case 11

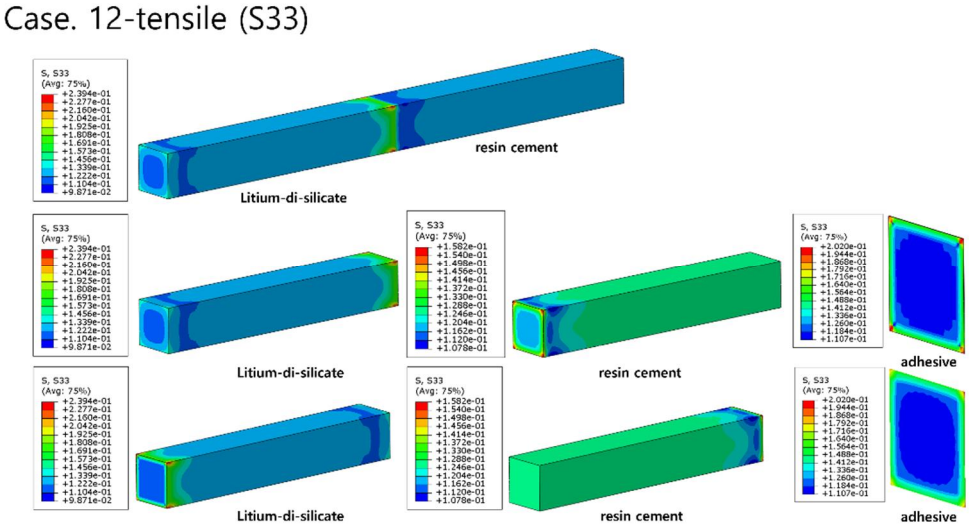

Fig. 38. Normal stress distribution under tension in Case 12

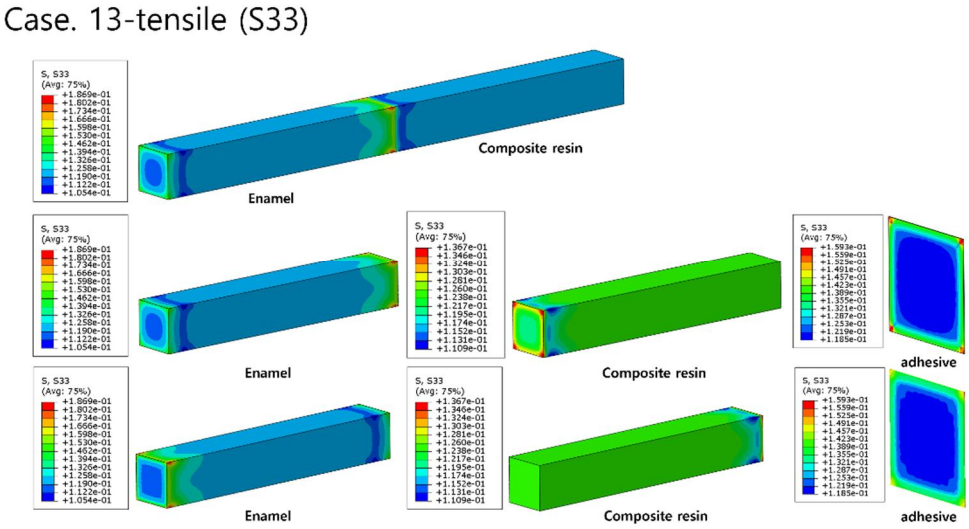

Fig. 39. Normal stress distribution under tension in Case 13

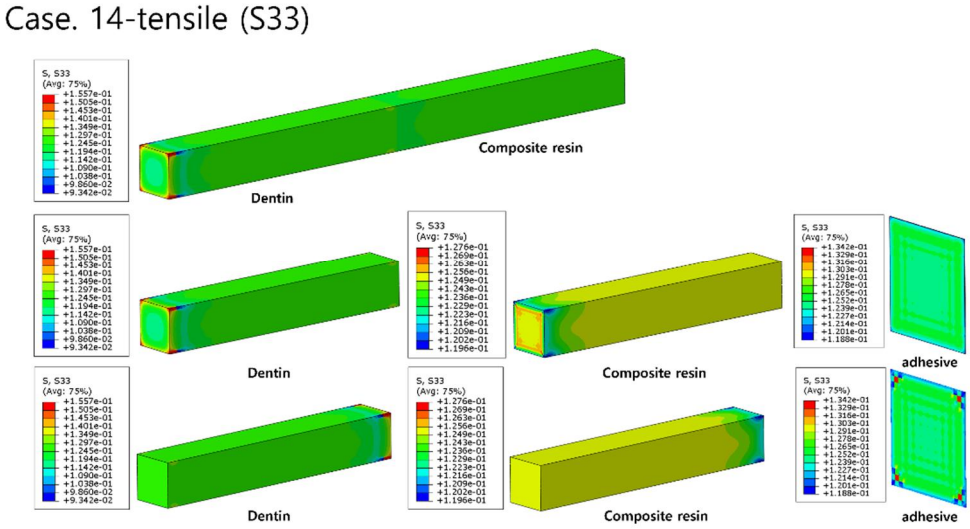

Fig. 40. Normal stress distribution under tension in Case 14

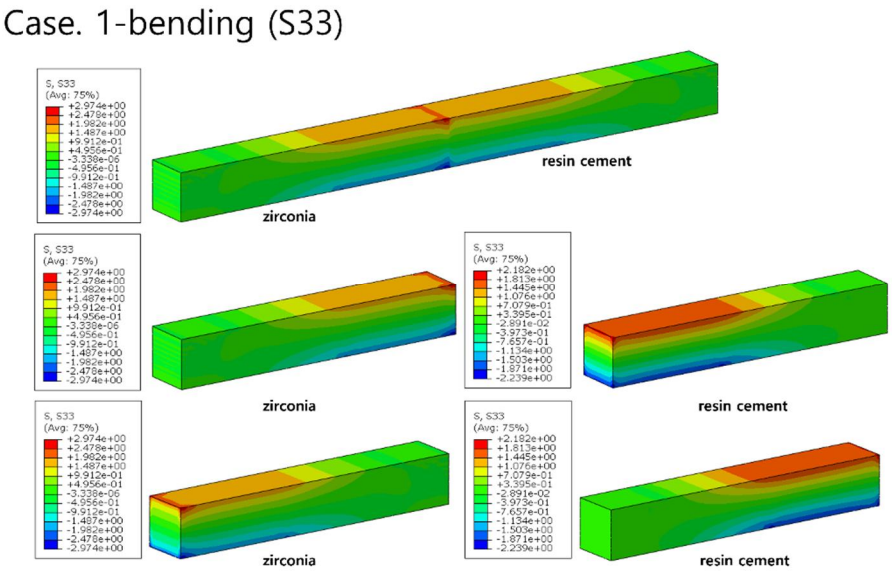

Fig. 41. Normal stress distribution under 4-point bending in Case 1

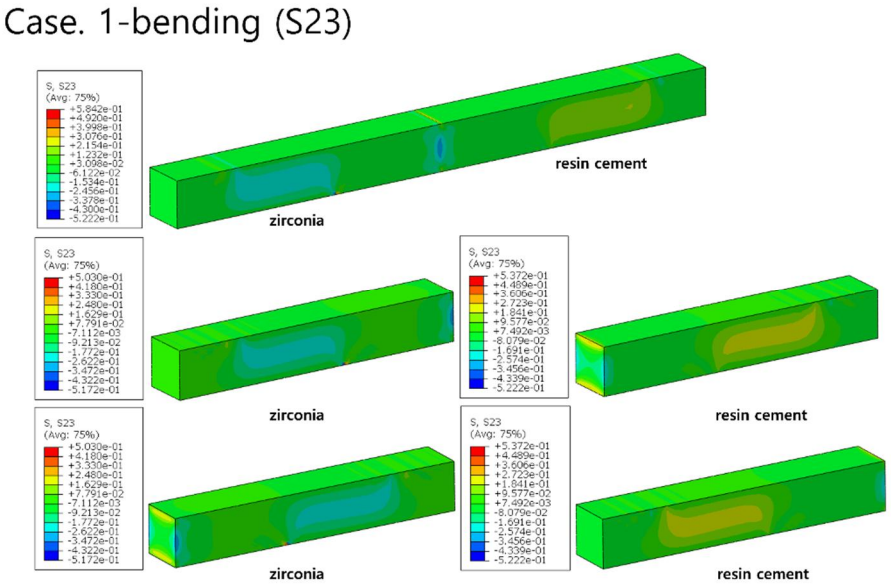

Fig. 42. Shear stress distribution under 4-point bending in Case 1

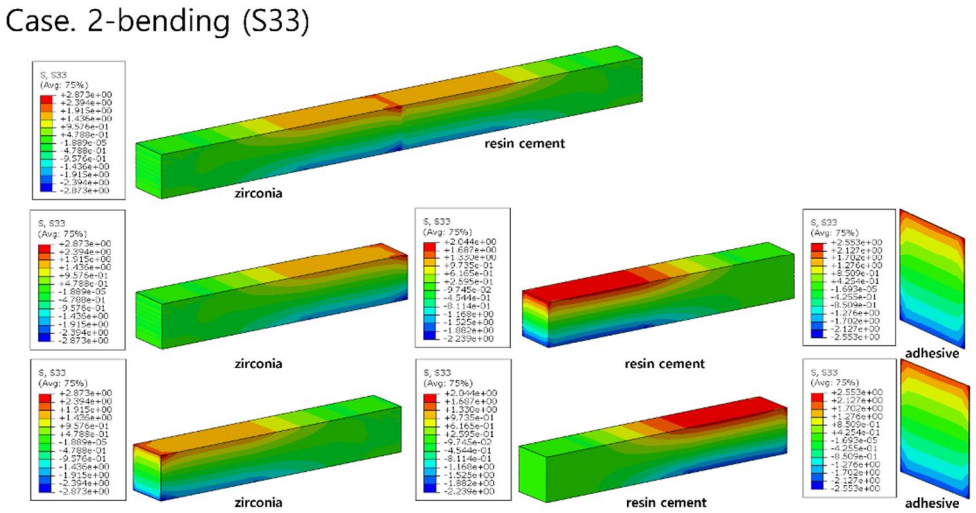

Fig. 43. Normal stress distribution under 4-point bending in Case 2

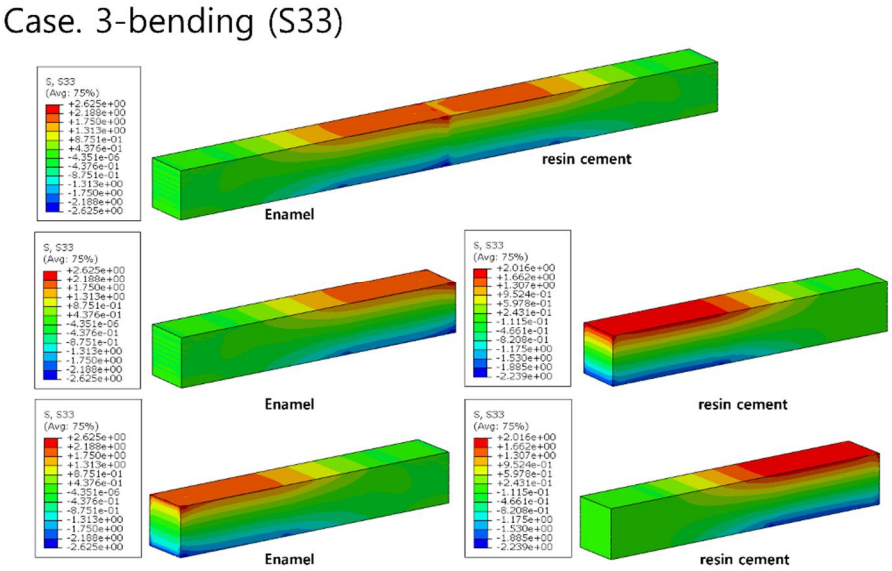

Fig. 44. Normal stress distribution under 4-point bending in Case 3

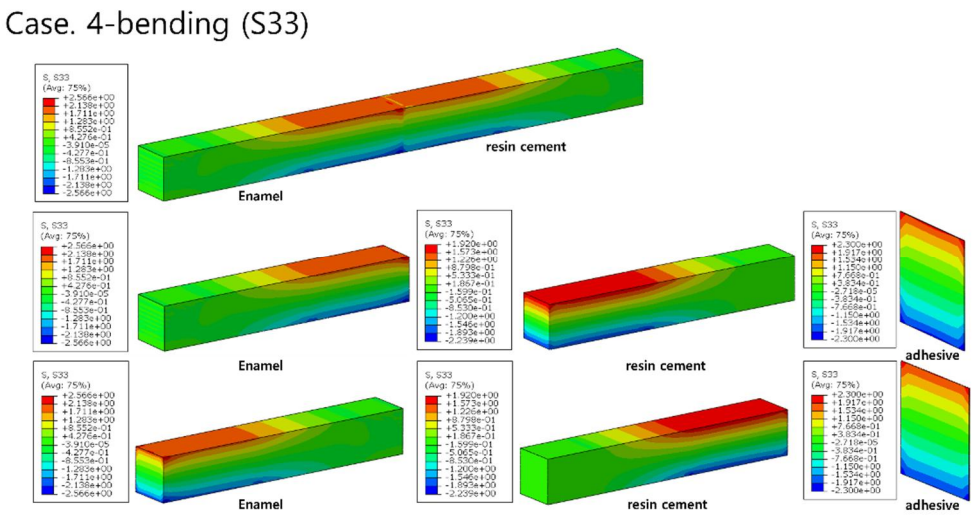

Fig. 45. Normal stress distribution under 4-point bending in Case 4

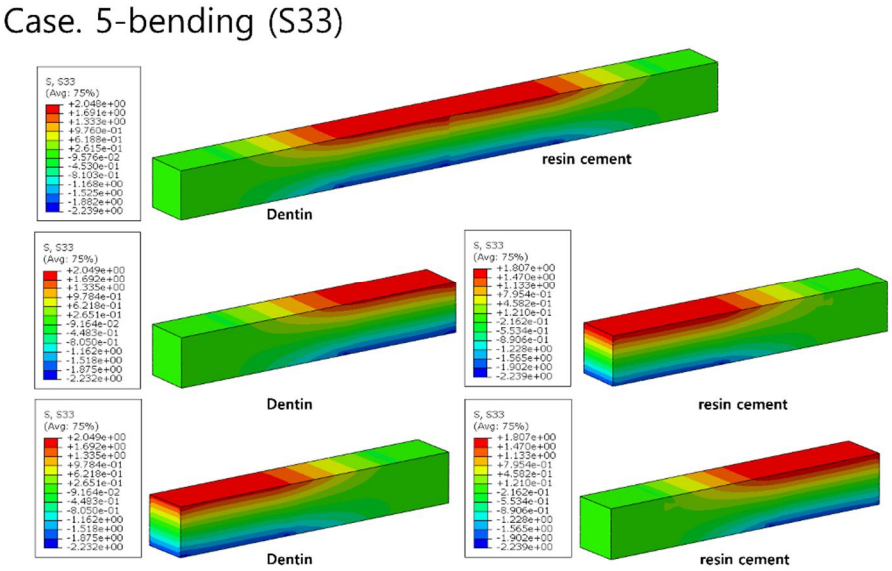

Fig. 46. Normal stress distribution under 4-point bending in Case 5

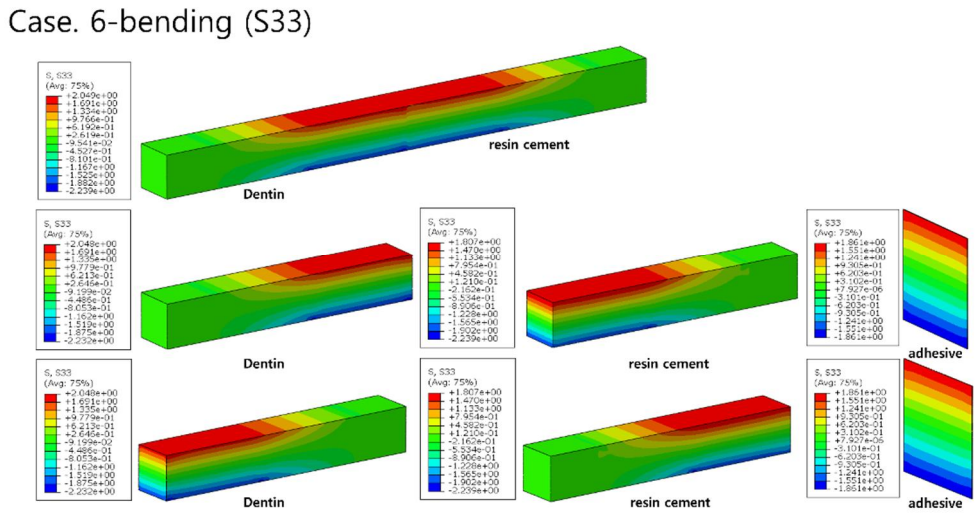

Fig. 47. Normal stress distribution under 4-point bending in Case 6

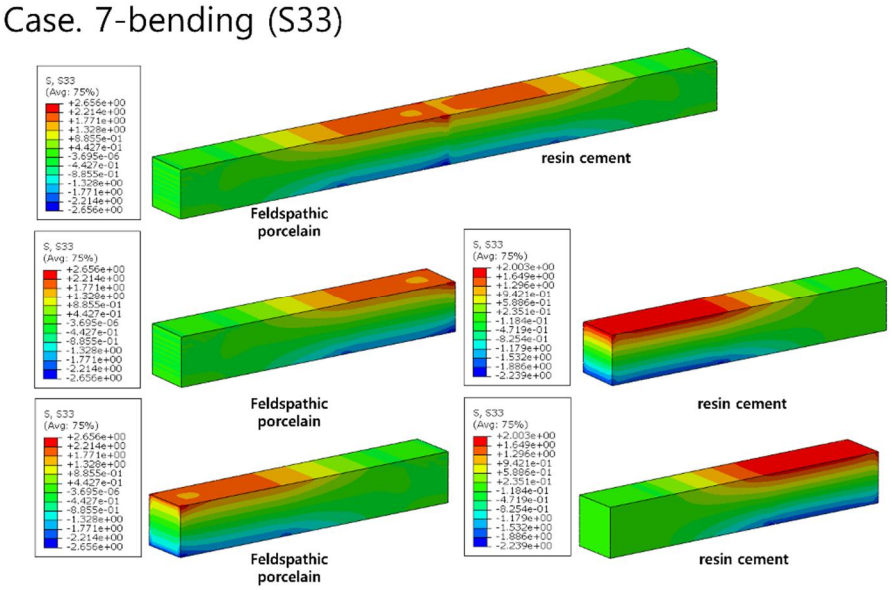

Fig. 48. Normal stress distribution under 4-point bending in Case 7

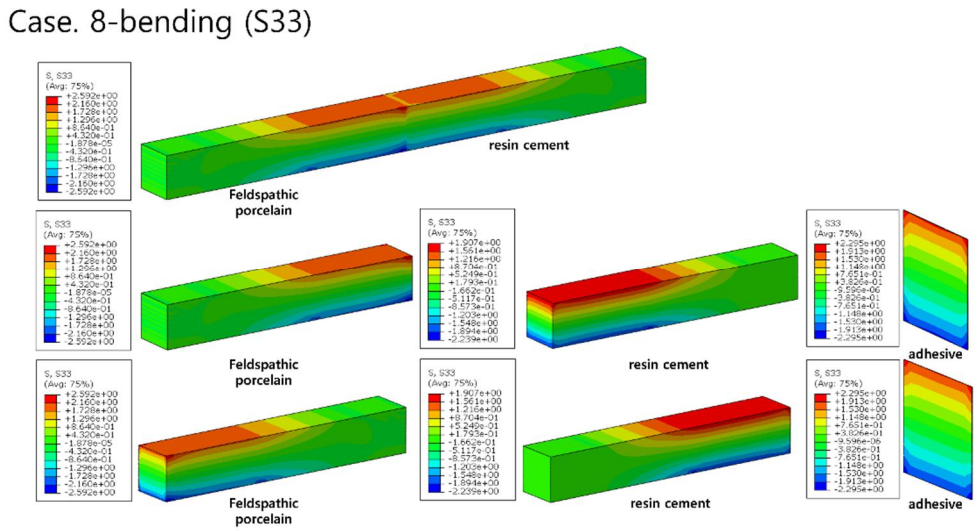

Fig. 49. Normal stress distribution under 4-point bending in Case 8

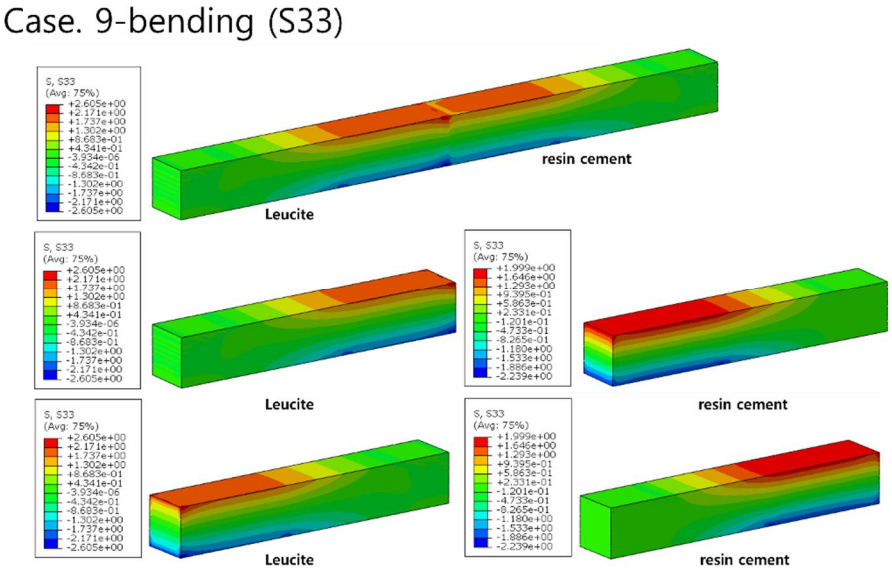

Fig. 50. Normal stress distribution under 4-point bending in Case 9

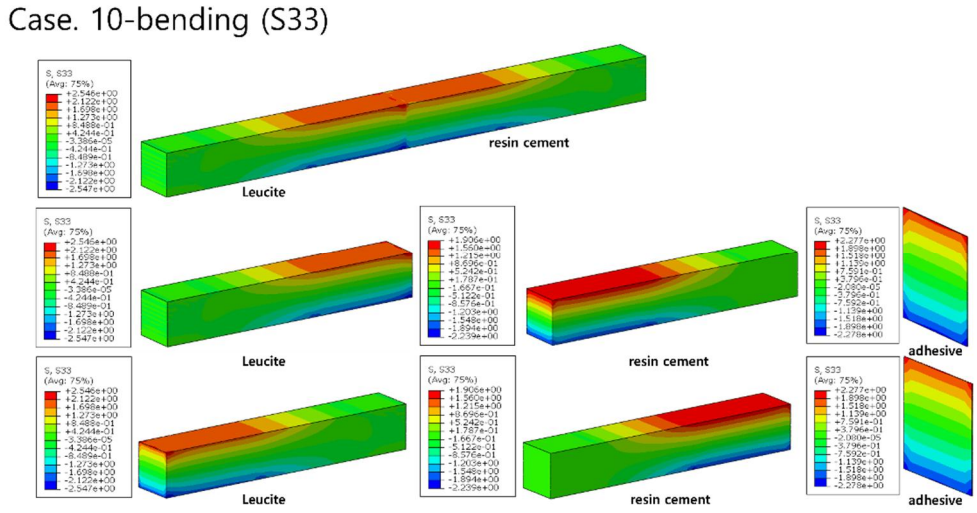

Fig. 51. Normal stress distribution under 4-point bending in Case 10

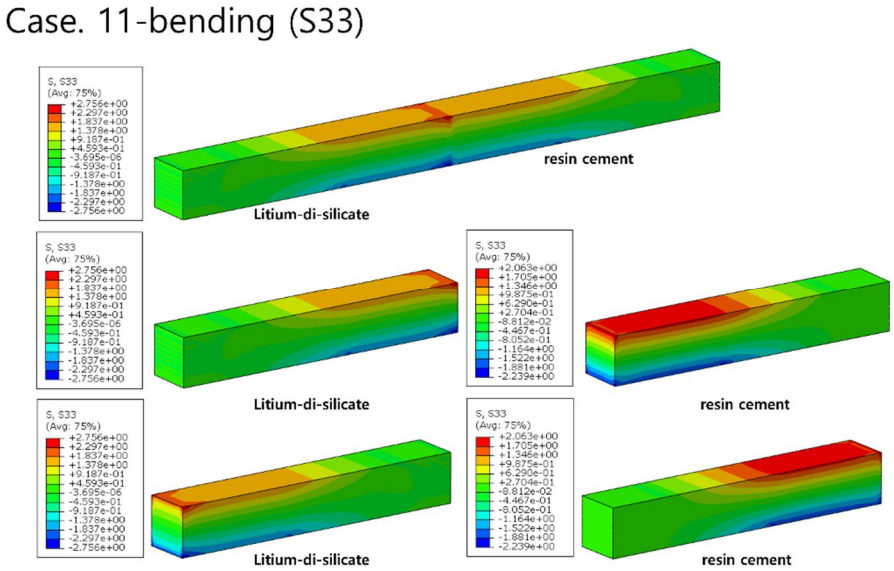

Fig. 52. Normal stress distribution under 4-point bending in Case 11

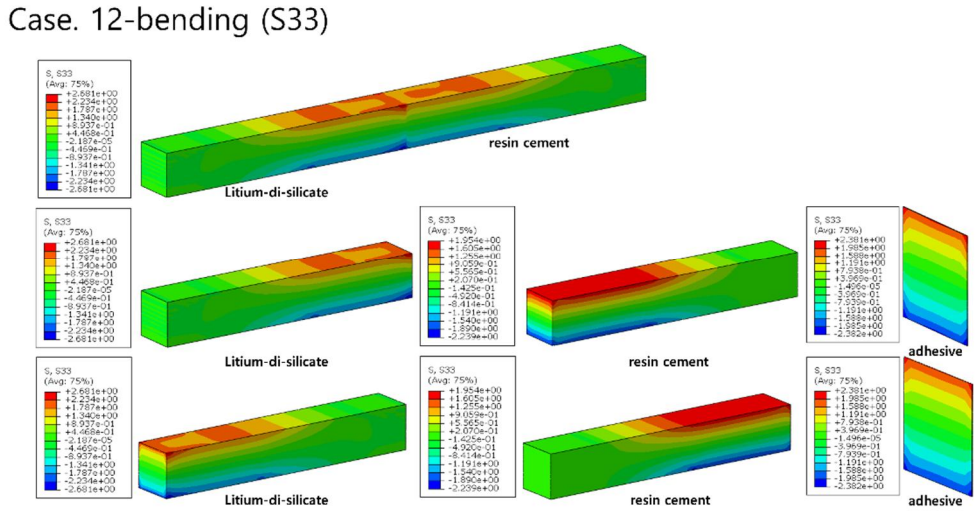

Fig. 53. Normal stress distribution under 4-point bending in Case 12

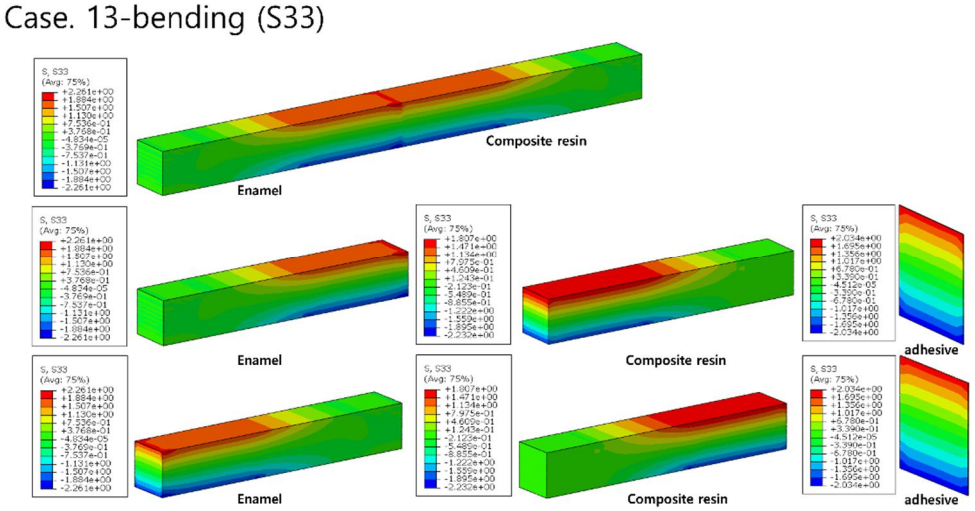

Fig. 54. Normal stress distribution under 4-point bending in Case 13

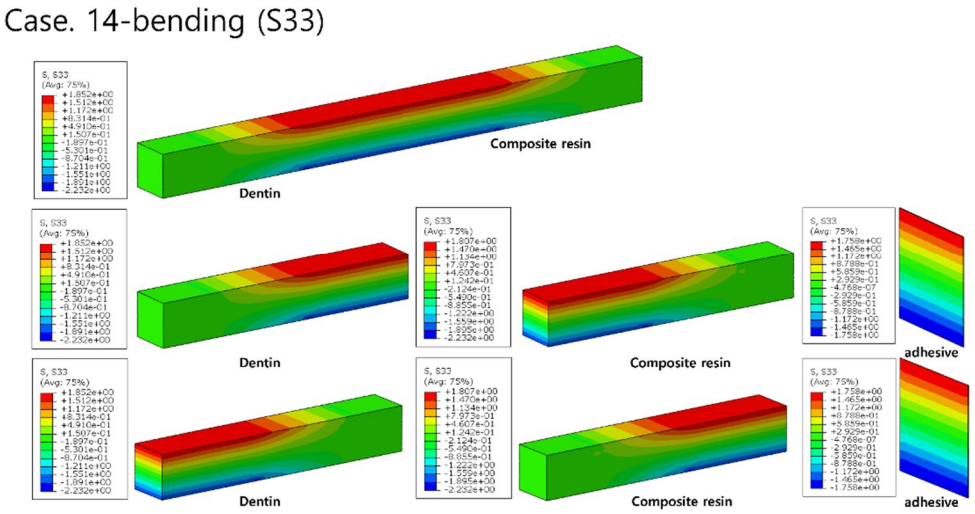

Fig. 55. Normal stress distribution under 4-point bending in Case 14